Spatio-temporal drought characteristics in the Limpopo basin from 1918 to 2018
- ## A case study based on analysis of the Standardized Precipitation Evaporation Index (SPEI)

Sandra Domingos Sambo

Sandra Domingos Sambo (2021).
Spatio-temporal drought characteristics in the Limpopo basin from 1918 to 2018
-   A case study based on analysis of the Standardized Precipitation
Evaporation Index (SPEI)
Master degree thesis, 30 credits in *Subject of degree*
Department of Physical Geography and Ecosystem Science, Lund University

Level: Master of Science (MSc)

Course duration: *September* 2020 until *January 2021*

Spatio-temporal drought characteristics in the Limpopo basin from 1918 to 2018
-A case study based on analysis of the Standardized Precipitation Evaporation Index (SPEI)

Sandra Domingos Sambo

Master thesis, 30 credits, in *Geomatics*

Supervisors:

Andreas Persson

Department of Physical Geography and Ecosystem Science,

Lund University

Petter Pilesjö

Department of Physical Geography and Ecosystem Science,

Lund University

Exam committee:

Virginia Garcia
Department of Physical Geography and Ecosystem Science,
Lund University

Acknowledgements

Abstract

The identification of the characteristics of drought are of great importance in water resources planning and management. This study explored the characteristics of drought at Limpopo River Basin (LRB) from 1918 to 2018. Two time scales were used; they were the 3-month and 12-month time scales using the Standardized Precipitation Evaporation Index (SPEI), with the aim of studying the characteristics of drought over the past 100 years, analyzing its onset, termination, duration, severity, intensity and frequency. A python script based on the run theory method was used to determine the characteristics of drought in the study area. The results show that in the Limpopo River Basin (LRB) the onset and termination of drought are difficult to determine due to the complexity of the phenomena, however the beginning of drought tended not to start at a specific season while the cessation of the drought tended to end during spring or autumn.

The number of droughts that last 3 months and 12 months in 100 years varies from 137 to 148 droughts and from 32 to 37 droughts respectively. The highest number of droughts was registered in South Africa and the lowest number of droughts was registered in Mozambique and Zimbabwe. The severity of the droughts in the region was also evaluated. The most severe droughts were registered in the years 1941-1942, 1946-1947, 1947-1948, 1963, 1972-1973, 1982-1983, 1990-1993, 2005-2006 and 2015-2016. Those droughts affected the entire basin or the major part of it.

Further analysis about drought trends and correlation with NDVI is also analyzed in this study. The Mann-Kendall trend test analysis was used to analyze the trends of drought in the seasonal and annual scales. The results of the non-parametric Mann-Kendall trend test applied to SPEI 12-month scale indicate increasing in drought in the entire Limpopo River Basin region. The 3-month SPEI time scale was used to analyze seasonality of trends over the study area. Each country within the LRB experienced different drought transitions through the seasonal SPEI analysis, with the winter being the one with the greatest increase in drought trends.

The response of vegetation to drought was evaluated by examining the correlation of the SPEI with the NDVI vegetation index from satellite images. The results suggest that the 12-month SPEI was found to have the best correlation with NDVI for the majority of the stations. However, the 3-month SPEI has also a high correlation with SPEI, but the correlation between NDVI and SPEI varies significantly between seasons. The highest correlations occurred during spring and

autumn and lower correlations were observed during summer and winter for the majority of the stations.

Abbreviations

AppEEARS - Application for Extracting and Exploring Analysis Ready Samples

DJF – December, January and February

EOS – Earth Observing System

FAO – Food and Agriculture Organization

JJA – June, July and August

LPDAAC - Land Processes Distributed Active Archive Center

LRB – Limpopo River Basin

MAM – March, April and May

MK – Mann-Kendall

NASA – National Aeronautics and Space Administration's

NDVI – Normalized Difference Vegetation Index

PET – potential evapotranspiration

PM - Penman–Monteith

SPEI – Standardized Precipitation Evapotranspiration Index

SPI – Standardized Precipitation Index

SON – September, October and November

WHO – World Health Organization

Contents

1. Introduction

Water scarcity has frequently been occurring in many parts of the world; partly because the demand for water has dramatically increased due to population growth and expansion of the energy, agricultural and industrial sectors, and partly because of climate change and contamination of water supplies (Belal et. al, 2014; El-Ramady, Mohamed & Saleh, 2014). In the Limpopo River Basin (LRB) located in the southern part of Africa, water scarcity is the result of the highly variable climate, characterized by extreme seasonality, intense El Niño Southern Oscillation (ENSO) events, and interactions with the oceanic climates of the Atlantic and Indian Oceans, which make precipitation and runoff highly variable in the basin (Mosase and Ahiablame 2018). According to Kandji et al., (2006) ENSO events have been linked to drought and flooding in southern Africa. Drought is the significant absence of precipitation from normal over an extended period of time, causing water shortage for some activities, groups, or environmental sectors (Hayes et al., 2010 and Bae et al., 2018).

Drought affects more people than any other hazard, and is considered to be the most complex but least understood of all natural hazards (FAO 2008; Iviescas et. al, 2019). In recent decades, large scale intensive drought has been observed in all continents, affecting severely large areas across the world (Wang et al., 2018). Southern Africa is also suffering various drought incidents causing devastation, including livestock deaths, human losses and crop failures at different spatiotemporal scales (Mo and Lyon, 2015). Additionally, in Southern Africa, drought has a direct impact on water supplies affecting food security and energy supplies of millions of people (NASA, 2019). The International Federation of Red Cross and Red Crescent (IFRC, 2019) reported that in southern Africa at least 11 million people are facing food shortages due to drought.

The Limpopo River Basin (LRB) is a drought vulnerable region, as the rainfall is very irregular and unpredictable, especially in the rainfed agricultural areas that are characterized by low and erratic precipitation (Leira et al., 2002; FAO 2004; Gebre and Getahun, 2016). Several studies have been performed to evaluate drought impact in the Limpopo River Basin. Most of these studies focus on the Standardized Precipitation Index (SPI) to analyze the characteristics of drought over the region and most of them investigate drought in a country - regional perspective. One example is Brito and Julaia (2007) who analyzed drought characteristics based on SPI to analyze spatial and temporal drought distribution. Gebre & Getahun (2016) also analyzed

climate variability and drought frequency events in the Limpopo River Basin, South Africa. Even though most research has focused on the SPI index to analyze characteristics of drought in the Limpopo River Basin, none of them have applied the Standardized Precipitation Evaporation Index as a main indicator of drought in the study area. In addition, none of them provides an analysis of long term drought. Therefore, this study is the first of its kind to provide a spatial and temporal study of the characteristics of drought in the Limpopo River Basin based on SPEI. According to Vicente-Serrano et al. (2010) and Tong et al. (2018), it is difficult to quantify the characteristic of drought in terms of intensity, magnitude, duration and spatial extent. This is due to the lack of clear boundaries (large affected areas of these events), high frequency and long duration, since drought often develops slowly over months or years (Schwab 2013; Tong et al. 2018). Therefore, a number of indices were developed to quantify, analyze and monitor drought, thus allowing the drought to be quantified in order to study its characteristics. Among several drought indices, the Standardized Precipitation-Evapotranspiration Index (SPEI), developed by Vicente-Serrano et al. (2010), is a relatively new index that can be applied to drought studies (Pathak & Dodamani, 2019). This index allows for monitoring the intensity and spatial extent of droughts at different time scales. This study is focused on finding the characteristics of drought such as severity, intensity, onset, termination, duration, and frequency based on the SPEI global dataset from 1918 to 2018. A trend analysis based on the Mann-Kendall test is also performed on the historical data in order to analyze drought trends over the Limpopo River Basin. In addition, a correlation analysis between NDVI, based on MODIS vegetation index product, and SPEI is performed. It is crucial to monitor and analyze historical drought events as they increase our understanding of the phenomena. This can help us to know when drought starts and ends so that drought planners can decide when to start implementing water conservation or mitigation measures (Sonmez et al., 2005).

1.2.   Objectives and Research Questions

This study aims to analyze drought characteristics in the Limpopo River Basin, such as onset, end, duration, severity, intensity, frequency and trends, based on the SPEI (Standardized Precipitation Evapotranspiration Index) between 1918 and 2018. In addition, the study aims to investigate the performance of the drought index based on

Normalized difference vegetation index (NDVI). The study will observe the seasonal (3-month SPEI) and annual (12-month SPEI) variation of obtained data from the SPEI dataset on the region of interest based on nine (9) distributed stations along the different regions of the basin, to answer the following research questions:

- What is the most frequent season for drought start and end in the Limpopo River Basin?
- What is the frequency of drought in the past 100 years over the study area, and which part of the basin is most prone to drought?
- In which years did the most severe droughts occur in the Limpopo basin?
- How does the SPEI vary annually and seasonally and what is the trend in the study area?

- How does vegetation respond to drought index (SPEI) from 2001 to 2018 in the LRB?

2. Background

2.1. Drought definition

Among all the natural disasters, drought is responsible for vast losses in many sectors of human activity, particularly in agriculture. Its characteristics are quite different from other natural disasters. Earthquakes, floods and cyclones have a relatively immediate onset, duration and restricted geographical extent (Wilhite, 2000). On the other hand, drought starts slowly, can cover an extensive geographical area and has a long duration (Vaz, 1993). One of the main obstacles to drought investigation is the lack of general acceptance of a precise and objective definition of drought (Yevjevich, 1967). However, when defining a drought, it is important to distinguish between conceptual and operational definitions (Whilhite and Glantz, 1985). Conceptual definitions help to understand the meaning of drought and its effects (e.g. a drought is a long dry period), while the operational definitions, on other hand, attempt to identify drought's onset, termination, and severity.

The character of drought varies in different climates and its impact depend on the local environmental and socio-economic characteristics (Wilhite et al., 2016). These facts contribute to the lack of a rigorous and universal definition of drought. The drought itself is due to deficiency in rainfall, which over time affects other

important sectors, especially water resources and agriculture, causing other impacts such as economic, social and environmental impacts, and operates on many different time scales (FAO, 2016). Palmer (1965) defines drought as a significant deviation from the normal hydrologic conditions of an area. While for Linseley et al. (1959) drought is a sustained period of time without significant rainfall. There are many definitions of drought, depending on its type in terms of precipitation, soil moisture or potential evapotranspiration (Bae et al., 2018). Thus, Wilhite and Glantz (1985) describe four types of drought, specifically meteorological, agricultural, hydrological and socio-economic drought.

- Meteorological drought is defined as the lack of precipitation, as compared to a normal or average conditions, over a region for an extended period of time. The definition of meteorological drought can vary depending on the region, since the atmospheric condition resulting in deficiencies of precipitation are region-specific.

- Agricultural drought refers to a period with a reduction in soil moisture availability below the ideal level required by a crop to develop during the different growth stages, leading to impaired growth and reduction of yields. This type of drought can expose plants to water stress, affecting pastures and rain-fed crops.

- Hydrological drought refers to the impact of rainfall deficits on the water supply, and occurs when a meteorological drought reduces the availability of natural and artificial surface and subsurface water resources.

- Socio-economic drought occurs when human activities are affected by reduced precipitation. This type of drought is based on the impact of drought conditions with elements of meteorological, agricultural and hydrological drought associated to the supply and demand of some economic good such as vegetables, grain, fruits and meat.

Generally, meteorological drought starts first, followed by the agricultural, then hydrological types. This study is investigating the 3-month SPEI timescale that is useful for the analysis of agricultural drought and the 12-month SPEI timescale that is important for the analysis of hydrological drought (Alsafadi, 2020).

2.2.   Drought in the Limpopo River Basin

In several dry regions of the world, water scarcity has become a limiting factor for economic development (Zhu and Ringler, 2010). The Limpopo River Basin in

Southern Africa is such a region; the region is prone to drought, due to low rainfall accumulation during the growing season.

In Africa, drought has caused much devastation, including livestock deaths, crop failures and human losses at varying spatiotemporal scales (AghaKouchak 2015, Haile et al.,2019). The emergency events database (EM-DAT, 2014) reported that at least 847 143 people have been killed by drought in Africa during 1900 to 2013, with 362 225 799 people affected causing a damage of around 2 920 593 000. 00 USD.

In Southern Africa, 60% of the area is vulnerable to drought, with 30% highly vulnerable (IFAD 1996; Beson et al. 1997). The region has experienced some of the most damaging drought ever recorded, affecting a large area of southern Africa. For example, the 1991-92 drought affected approximately 86 million people, of which 20 million were severely affected, resulting in a deficit of cereal supplies of more than 6.7 million tons (SADCC 1992; Wilhite 2000; Mosase and Ahiablame, 2018). In the last decades, droughts become more frequent in the Limpopo River Basin (Gebre & Getahun, 2016). The watershed has experienced severe droughts alternating with floods, with 1.2 million people needing immediate food assistance in 2016 due to drought that caused 100% of crop losses in some areas (Merz, 2020). The 2005-2006 drought damaged 72.500 hectares of cultivated cropland in Botswana, resulting in economic losses (Mosase, 2018). Additionally in the past, the basin has experienced major droughts and is, at times, a basin under water stress, affecting millions of people, with some of the worst droughts occurring in 2003, 2002, 1995, 1994, 1992, 1991, 1987, 1984, 1983, 1981 and 1980 (WHO 2012; Mosase and Ahiablame 2018; Merz 2020). In the region, drought is a regular phenomenon that occurs every 7 to 11 years, with extreme droughts occurring every 10 to 20 years (Leira et al, 2004 and FAO 2004).

Droughts in the Limpopo basin are complicated due to the disparities in climate and rainfall distribution, with most of its watershed under semi-arid conditions (WMO, 2012). According to Gebre and Getahun (2016), drought impact is more persistent in arid and semi-arid regions. Furthermore, the impacts of drought in the basin are aggravated by land degradation, climate change, deforestation and growing water demand (IPCC, 2013; Masih and Maskey, 2014). Additionally population growth, agricultural activities, industrial development, and urbanization place pressure on the water resource in the basin (Mosase and Ahiablame, 2018).

2.3. Drought indices

The difficulty on the identification of drought characteristics, in terms of duration, intensity, magnitude and spatial extent (Vicente-Serrano, 2010), have resulted in efforts to develop drought indices for analyzing and monitoring drought. Drought indices are used to quantify and compare drought severity, duration and extent across regions with different climatic and hydrological regimes (Stagge et al., 2015). A number of indices have been developed throughout the years to quantify, monitor and analyze drought severity (Heim, 2002). Such indices are usually based on combination of climate and meteorological variables, with precipitation as the most important variable in defining the magnitude and intensity of drought (Heim, 2002). The most commonly used indices for drought analysis and monitoring are the Palmer Drought Severity Index (PDSI) (Palmer, 1965) based on a soil-water balance equation, and the Standardized Precipitation Index (SPI), based on a precipitation probabilistic approach. The main critic of using SPI as an index for drought monitoring is that the method is based only on precipitation data. The index does not consider other variables that can influence drought such as temperature, evapotranspiration, wind speed and soil water capacity (Vicente-Serrano et al., 2012). This means that droughts are only controlled by the variation of precipitation. However, it is important to consider other variables, such as temperature and potential evapotranspiration, to define the characteristics of drought. Vicente-Serrano et al. (2010) related the importance of including temperature as a variable to define drought. According to Vicente-Serrano et al. (2010), empirical studies have shown that high temperatures affect the severity of drought. For that reason, the PDSI index, which includes temperature data, is preferable, especially when the study involves a future climate scenario. However, the PDSI lacks the multi-scalar character that is important for assessing drought in relation to different drought types and different hydrological systems. Because of the limitations of SPI and PDSI, the Standardized Precipitation Evapotranspiration Index (SPEI) that includes information describing precipitation and potential evapotranspiration has been formulated to analyze drought severity; the index combines the sensitivity of PDSI and SPI. SPEI is a multi-scalar characterization; this allows the identification of different types of drought and impacts in the context of global warming. Besides, the SPEI index can be used to identify and analyze drought severity in any climate region of the world and can be used for possible effects of temperature variability (Wang, 2018).

2.3.1. Standardized precipitation evapotranspiration Index

The Standardized Precipitation Evaporation Index (SPEI) was first proposed by Vicente-Serrano et al. (2010) as an index that can be used detect, monitor and analyze drought in different climate regions (Zhang et al., 2020), but also detects whether drought occurs and reflects its duration over multiple time scale. SPEI permits the comparison of drought severity over time and space, since it can be calculated for a wide range of climates. In addition, the SPEI can be used to measure drought severity according to its intensity and duration, and can be used to identify the onset and end of drought episodes (Vicente-Serrano et al., 2010).

The SPEI is an essential index in terms of drought characterization and climate change monitoring since it also takes into consideration both temperature and potential evapotranspiration (Alsafadi, 2020; Spinoni et al. 2013; Li et al. 2012). A number of equations exist to model potential evapotranspiration (PET) based on available data, among them, the most used equations to compute PET are: The Thornthwaite equation and the Penman-Monteith equation (Chen, 2018). SPEI is not linked to any particular PET equation; the usage of any particular one of them depends on the available data. The original version of the SPEI is based on the Thornthwaite equation (Thornthwaite, 1948) for estimation of PET. However, Chen (2018), Penman (1948) and Monteith (1965) related that the changes in the PET estimated using the Penman–Monteith method displays better agreement than the Thornthwaite method since the Penman–Monteith approach considers humidity, solar radiation, and wind speed, and based on these variables it is possible to capture the magnitude of evapotranspiration. The Thornthwaite equation only requires the latitude of the site and the mean daily temperature, and it is used when there is limited data availability. In addition, previous investigations have indicated that the Thornthwaite equation underestimated evapotranspiration in arid and semiarid regions (Jensen 1990; Bae et al., 2018), and overestimated evapotranspiration in tropical and humid equatorial regions (van der Schrier et al., 2011; Bae et al., 2018). The conditions found in the LRB are typical of those found in arid and semi-arid regions.

The Food and Agriculture Organization (FAO) recommends the use of the Penman-Monteith equation for the calculation of evapotranspiration because the equation uses all the parameters that govern energy exchange and the corresponding latent heat flow (evapotranspiration) from uniform vegetation extensions (Chen,

2018). The Penman-Monteith (PM) method is considered to be among the best physically based formulas in the world (Chen, 2018). A grid SPEI dataset for 1901 to 2018 based on the Penman-Monteith method is available (Dikshit, 2020. An R-package is available for calculating the SPEI from user-selected input data using the Thornthwaite, Penman-Monteith, or Hargreaves methods. Therefore, the SPEI (http://sac.csic.es/spei), which calculates PET through the PM equation, is used in this study.

Calculation of SPEI

SPEI is a multi-scalar drought index that combines data of precipitation and temperature. The SPEI is calculated based on monthly or weekly difference (D) between precipitation (P) and potential evapotranspiration (PET). The difference (D) provides a measure of the water surplus or deficit for the analyzed month (i), and is calculated according to Equation (1):

$$D_i = P_i - PET_i$$

<div align="right">Equation 1</div>

As in this study, the used SPEI was calculated by applying the Penman-Monteith method, equation 2, to calculate PET. It requires daily, weekly and monthly meteorological data, including air temperature, humidity, sunshine duration and wind speed to perform the calculation.

$$PET = \frac{0.408\Delta(R_n - G) + \gamma(\frac{900}{T} + 273))u_2(e_s - e_a)}{\Delta + \gamma(1 + 0.3u_2)}$$

<div align="right">Equation 2</div>

Where: Δ is the slope of the vapor pressure curve; R_n is the net surface radiation; G is the soil heat flux, γ is the psychrometer constant; u_2 is the wind speed at 2 meters and (e_s - e_a) represents the saturated vapor pressure.

The calculated D_i values (equation 1), are aggregated over different timescales. The difference $D_{i,j}^k$ in a given month j and year i, depends on the chosen time scale k, is calculated based on the following equation.

$$D_{i,j}^k = \sum_{l=j-k+1}^{j} D_{i,l} \ , \ if \ j \geq k$$

<div align="right">Equation 3</div>

The water balance is then normalized using the log-logistic distribution to calculate an SPEI time series.

$$f(x) = \frac{\beta}{\alpha}\left(\frac{x-\gamma}{\alpha}\right)^{\beta-1}\left(1+\left(\frac{x-\gamma}{\alpha}\right)^{\beta}\right)^{-2}$$ Equation 4

Where α, β, and γ are scale, shape and origin parameters, respectively, that can be obtained using the L-moment procedure. Parameters of the log-logistic distribution can be obtained following different procedures. More details about the log-logistic parameters can be found in Vicente-Serrano et al., 2010.

The log-logistic distribution adapts very well the D series for all time scales. The probability distribution function of the D series according to the log-logistic distribution is then defined as:

$$F(x) = \left[1+\left(\frac{\alpha}{x-\gamma}\right)^{\beta}\right]^{-1}$$ Equation 5

According to Vicente-Serrano et al., (2010) values of F(x) for the D series at different time scales adapt very well to the empirical F(x) values at different time scale of the analysis and climate characteristics.

Having F(x), the SPEI can be calculated as the standardized value of F(x) Abramowitz and Stegun (1965):

$$SPEI = W - \frac{C_0+C_1W+C_2W^2}{1+d_1W+d_2W^2+d_3W^3}$$ Equation 6

Where:

$W = \sqrt{-2\ln(P)}$ for P≤0.5, and P is the probability of exceeding a determined D value (Vicente-Serrano et al., 2010). If P≤0.5, p=1-F(x); if p>0.5, p is replaced by 1-p. The constants are C_0=2.515517; C_1=0.802853; C_2=0.0103228; d_1=1.432788; d_2=0.189269; d_3= 0.001308.

The SPEI can be calculated for any time scale (i.e. for 1-, 3-, 6-, 9-, 12-, 24-, or 48-month time sale). For this study the 3- and 12-month scales are used; the SPEI was calculated for each month of time series of years at 3 and 12 months timescales. For this purpose, a new series was created for each month with the elements corresponding to the moving sum of precipitation and PET. For example, the 3-month SPEI calculated for March 2018 utilized the precipitation and PET of January 2018 through March 2018 in order to calculate the index. Likewise, the 12-month SPEI for December 2018 utilized the precipitation and potential evapotranspiration for January 2018 through December 2018.

The choice of the time scale depends on the objective of the study. For short-term or seasonal drought identification the 1-month up to 6-month SPEI is used, thus the 1-, 3-, or 6-month scale is related to agricultural drought, while a 9-, or 12-month

scale is used for monitoring hydrological drought (Tan et al., 2015 and Alsafadi, 2020). In this study, the 3- and 12-month SPEI time scale values are used for each station within the LRB for detecting droughts over a short and long-term interval.

The SPEI values for drought can be classified, as can be seen in Table 1 (Bae, 2018; Chen, 2018), and the values can be compared with other SPEI values over the time and space.

Table 1- Drought classification based on SPEI values

Drought Categories	SPEI
Non-drought	$\geq$ -0.5
Mild drought	(-1.0 – -0.5)
Moderate drought	(-1.5 – -1.0)
Severe drought	(-2.0 – -1.5)
Extreme drought	$\leq$-2.0

Strengths and limitations of SPEI

According to Vicente-Serrano (2005), the strengths of SPEI include the combination of multi-temporal aspects with information on precipitation and evapotranspiration, making it more useful for studies on climate change. SPEI is an index that requires only climatological information to describe the severity of the drought. The limitations of this method include the requirements for more data than other drought indices such as SPI. The SPEI is sensitive to the potential evapotranspiration (PET) calculation method; different evaporation methods can lead to different SPEI results. As with other drought indices, a long base period of at least 30 years should be used in which natural variability should be used.

2.4. The MODIS vegetation index (VI) products

Remote sensing sensors play an important role in detecting and managing droughts as they offer information on spatial and temporal scales (Brian *et al*., 2012; Abuzar et al., 2017). Vegetation indices are empirical measures of vegetation activity at the land surface. These indices are designed to enhance vegetation reflected signals from measured spectral responses by combining two or more wavelength bands usually in the red (0.6-0.7 μm) and near-infrared (NIR) wavelengths (0.7-1.1 μm)

regions. The MODIS VI products offer a consistent temporal and spatial time series of global vegetation conditions that can be used for monitoring changes and detect trends on vegetation. In addition, the data can be used to study vegetation patterns useful for droughts (Jenkerson et. al, 2010). The vegetation index maps are provided at a temporal resolution of aggregated 16-day and monthly intervals and at spatial resolutions of 250 m, 500 m, 1 km, and 0.05 deg. The data provide two VI products, specifically the Normalized Difference Vegetation Index (NDVI) and the Enhanced Vegetation Index (EVI). The NDVI product is a continuation of the existing NOAA-AVHRR series, which in cooperation with MODIS data, provides long-term data vegetation index data that is used for monitoring studies. The gridded VI Terra Moderate Resolution Imaging Spectroradiometer (MODIS) products use MODIS surface reflectance corrected for molecular, aerosols, and ozone absorption as input to the VI algorithms equations.

2.4.1. The response of vegetation to drought time-scales

Since the MODIS vegetation index products provide time series data for vegetation monitoring, these data can be used to monitor vegetation indices in order to analyze how vegetation responds to drought over time and space. Among all vegetation indices, NDVI is the most often used for monitoring drought all over the world (Hassan et al., 2018). According to Chuvieco (2009), NDVI can be used to capture the spatial and temporal aspects of vegetation dynamics. According to Ji and Peters (2013) there is a close relationship between vegetation vigor and soil moisture, especially in arid and semiarid areas like the LRB. In addition, Tucker and Choudhury (1987) related that NDVI could be used as a response variable to identify and quantify drought disturbance in semiarid and arid regions. NDVI can be used to access drought condition by directly comparing it to precipitation or drought indices (Ji and Peters, 2003). The formulation of NDVI is based on the ratio of the difference in near infrared (NIR) and red reflectance bands divided by their sum in order to minimize certain band-correlated noise and the influence of variations in diffuse irradiance, clouds and cloud shadows, topography, sun and view angles and atmospheric attenuation (Didan et al., 2015). NDVI values vary from -1 to 1, with low values corresponding to stressed vegetation.

According to Ciais Ph et al., (2001) and Vicente-Serrano (2012), it is crucial to understand the response of land vegetation to drought. Therefore, the response among vegetation types is a big issue since vegetation types have different characteristic response times. In this study, we will not focus on different types of vegetation to analyze the impact of vegetation to drought; only NDVI values are analyzed.

3. Materials and Methods

3.1. Study area

The Limpopo River Basin is located in the southern part of Africa between the latitudes of 20ºS and 26ºS, and longitudes of 25ºE and 35ºE (Fig. 1). Its catchment area distribution among South Africa, Botswana, Mozambique, and Zimbabwe is 45%, 20%, 20% and 15 %, respectively (WMO, 2012). South Africa uses 60% of the total water usage, the current distribution of water usage will become increasingly harder to sustain as Mozambique, Zimbabwe, and Botswana experience rapid urban growth and begin large scale national development projects (Midgley, 2013). The total catchment is approximately 408 000 km^2 (WMO 2012 and FAO 2004). The LRB flows for a distance of 1750 km from South Africa to the Indian Ocean in Mozambique (WMO, 2012). The Limpopo River is the second largest river in the southern Africa, which rises in the Witwatersrand plateau, not far from Johannesburg. Flowing between the border of South Africa and Botswana, then between South Africa and Zimbabwe before it flows through Mozambique in the north of Gaza province to flow into the Indian Ocean, near the city of Xai-xai (Milhano, 2008).

In this study, nine locations in the LRB were selected, as illustrated in Figure 1. Stations 1 and 2 are located in Mozambique, stations 3 and 4 are located in Zimbabwe, stations 5 and 6 are located in Botswana, and stations 7, 8 and 9 are located in South Africa. The topography in the basin varies from above 2000 meters above sea level in the mountain regions of South Africa to below 7 meters across the eastern coastal plains in Mozambique.
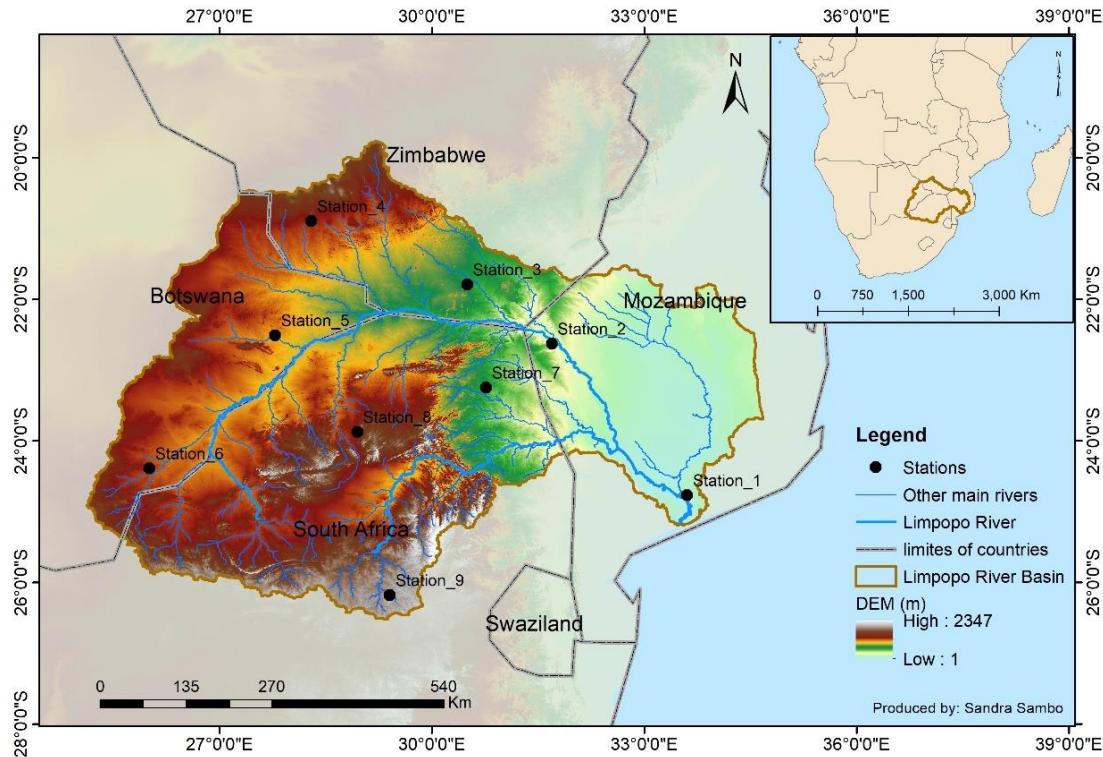
Figure 1. Location map of the study area and the 9 meteorological stations.

The population of Limpopo River Basin is estimated at 18.8 million, with 52% of people living in rural areas and 48% in urban areas (Merz et al., 2020). In the basin there are 102 dams and thousands of small-scale reservoirs and irrigation projects. Agriculture is mainly rain-fed, despite the high variability of rainfall (Mosase and Ahiablame, 2018). The total harvest area is 2.9 million hectares, and 91 percent of the area is cultivated under rainfall (Zhu, 2010). The region is highly dependent on rainfall to feed its increasing human population, implying that LRB is highly sensitive to drought events.

The LRB Watershed is home for several million people, distributed among the four countries, who uses water for industrial purposes, electricity production, domestic or agricultural use. Adverse climatic conditions reinforce the need for effective cross-border management of water resources, with effective governance structures and mechanisms for distribution and control of these resources (Merz, 2020).

Water usage in the LRB system is dominated by irrigation; the agricultural sector accounts for 60% of the total water usage, urban usage accounts for 30%, and the remaining demand is divided evenly across the rural, mining, and power sectors

(LBPTC, 2010). Although mining accounts for a smaller proportion of water use, it has caused environmental consequences via pollutants (Merz, 2020). In addition, in the coming years rapid growth is expected in urban population and mining energy projects, which should put enormous pressure on LRB water resources (Ashton et al., 2018).

3.1.1. Climate of the Limpopo River Basin

According to Köppen's classification, the climate of the basin is predominantly semi-arid, dry and hot (Bsh in Figure 2) (FAO-SAFR, 2004). The central valley of the river is arid, dry and hot (Bwh), the South African part of the basin is temperate (Cwc and Cwa) and the coastal plain of Mozambique is mainly temperate, with no dry season (Cfa). The average rainfall of the basin is 530 mm per year, ranging from 1200 mm per year in the southeast to 200 mm in the central-west (LBPTC 2010; Midgley et al. 2013; Gebre and Getahun 2016; Mosase and Ahiablame 2018). The climate is characterized by extremely variable rainfall, resulting in a mixture of very dry years and years with floods (Mosase and Ahiablame, 2018). Two distinct seasons characterize the region: the hot and humid season (October to March) and the dry and cold season (April to September). On the other hand, Mosase and Ahiablame (2018) distinguish four seasons along the LRB: Summer (January, February and March), autumn (March, April and May), winter (June, July and August) and spring (September, October and November). The areas that receive the highest rainfall are the mountainous areas in South Africa, while the lowest rainfall is usually found along the Limpopo River between Zimbabwe and South Africa (Gebre and Getahun, 2016). The precipitation in the Limpopo River Basin is very dependent on El Niño–Southern Oscillation (ENSO), giving warm and dry years during strong ENSO events (Wetterhall et al., 2015). ENSO refers to the changing of sea surface temperature in the equatorial Pacific Ocean affecting the regional climate in different regions of the world (Sithole, 2016).

The average daily air temperature in the basin varies from 0 °C in winter to 36 °C in summer (Mosase and Ahiablame, 2018). In summer daily temperature exceeds 40 °C, while in winter temperature may fall to below 0 °C (FAO, 2004).

Evaporation is a significant factor in the climate in the LRB, which varies from 800 to 2400 mm.year^{-1}, with a mean of 1970 mm.year[1] (Gebre and Getahun, 2016). Warmer western and central regions of the basin experience between 2600 and 3100

mm.year[1]. High levels of evaporation mean that soils dries out quickly, reducing the amount of water available to plants, thus increasing their vulnerability to drought (FAO, 2004).
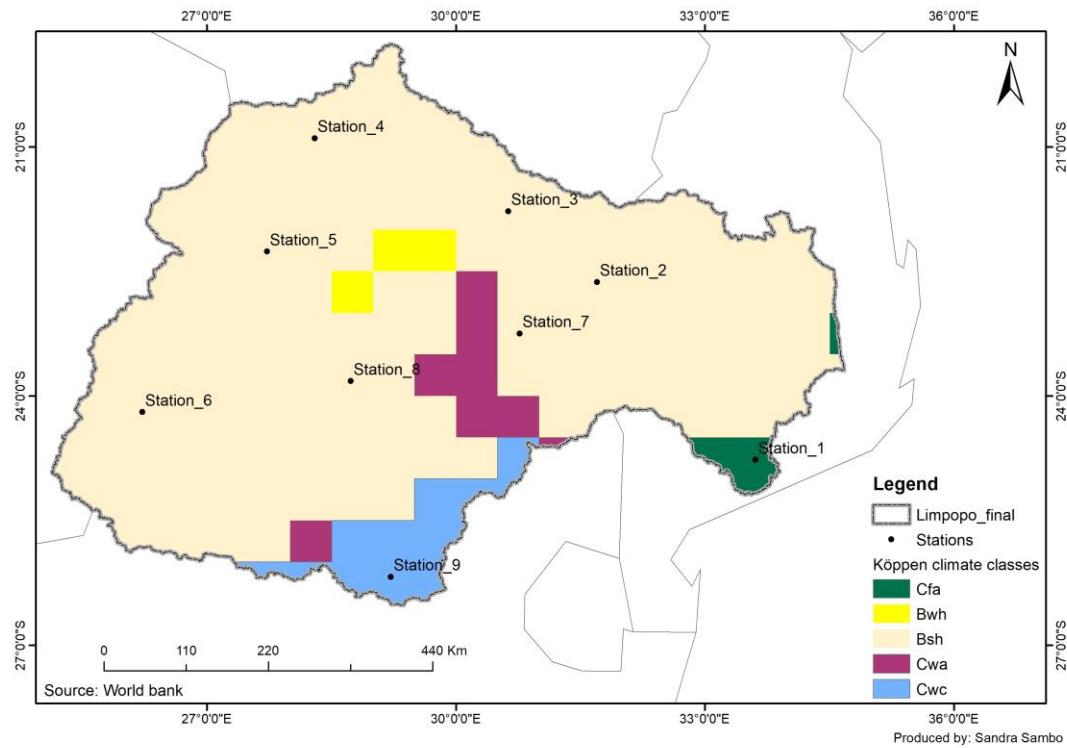
Figure 2. Köppen classification in the Limpopo River Basin. (Cfa – temperate with no dry season, Bwh – arid with dry and hot season, Bsh – semi-arid with dry and hot season, Cwa – humid temperate with dry winter and Cwc – temperate).

3.2.   Data

3.2.1. SPEI dataset

This study uses time series from the SPEI drought dataset from 1918 to 2018 over the Limpopo River Basin. The SPEI is a multiscale drought index based on monthly precipitation and potential evapotranspiration data and can be used to determine the onset, duration, and magnitude of drought conditions (Vicente-Serrano et al., 2010). The dataset used is a collection of imagery that offers information about drought condition at a global scale, which covers time scales from 1-48 months at a spatial resolution of 0.5 degrees (50 km) and provides temporal coverage for the period 1901-2018. The complete SPEI time series dataset is provided in Excel and NetCDF formats. According to Beguería et al., (2010), the SPEI dataset was generated from Climatic Research Unit (CRU) Time-series (TS) data. At the moment, the actual version is 4.04 (available at https://crudata.uea.ac.uk/cru/data/hrg/

15

cru_ts_4.04/cruts.2004151855. v4.04/): this is the most complete and updated dataset. The CRU-TS datasets provide climate variables including gridded precipitation, potential evapotranspiration (PET), vapor pressure, diurnal temperature range, minimum, maximum and mean temperatures, frost day frequency and cloud cover at the global scale, has a spatial resolution of 0.5° (Peng et al., 2020), and covers the period January 1901 - December 2019. The CRU TS datasets were produced using angular distance weighting (ADW) interpolation, based on monthly meteorological observations collected from ground stations all over the world (Peng et al., 2020). To evaluate the characteristics of droughts of seasonal and yearly timescale SPEI at 3-month and 12-month time scales were acquired from SPEI database (https://spei.csic.es/).

3.2.2. NDVI

Monthly long-term NDVI data from satellite imagery were used to study how vegetation responds to drought over the study area. The NDVI dataset was composed of the vegetation index (MOD13A3, collection v6) product of the Terra MODIS, which provides a value with 1 km spatial resolution and 1-month temporal resolution. NDVI was retrieved using the 16-days Maximum Value Composite (MVC) MODIS NDVI images, which use the pixel with the highest NDVI value. Each monthly MVC image is temporal averages of their two temporal MVC 16-day MODIS VI, weighted by the number of days between the monthly NDVI and biweekly MVC NDVI (Didan et al., 2015).

The MODIS collection is based on the Moderate Resolution Imaging Spectroradiometer (MODIS) data acquired by the National Aeronautics and Space Administration's (NASA) Earth Observing System (EOS). MODIS is suitable data for monitoring changes and detect trends on vegetation; this data can be used for study vegetation patterns useful for droughts (Jenkerson et. al, 2010). NDVI has been collected over the period of 2001 to 2018. The choice of the period for analyzing vegetation index is due to the fact that the MOD13A3 NDVI dataset only covers the period from 2000 to 2020, therefore for the year 2000 the data does not cover the month of January.

In this study, NDVI data corresponding to the same locations as the meteorological stations is used. The data were obtained with the help of the AppEEARS (Application for Extracting and Exploring Analysis Ready Samples) tool (AppEEARS, 2020)

available in LAPDAAC (https://lpdaac.usgs.gov/tools/appeears/). The tool allows the request of data based on point samples using geographic coordinate location (Didan, 2015). In the AppEEARS tool, a list that contains a set of coordinates was defined in order to download the time series of NDVI data, the coordinates were defined based on the location of the meteorological stations. The NDVI dataset was download from the NASA and EOS system (https://lpdaacsvc.cr.usgs.gov/appeears/). In the LPDAAC database the NDVI data can be downloaded in following formats: GeoTIFF, NetCDF and Excel files (Didan, 2015). The selected NDVI data from the LPDAAC Database was downloaded using AppEEARS tool in *.csv format.

3.3. Methodology

3.3.1. Drought Characterization

The method generally used for the identification of drought properties based on drought indices is the Run Theory, which has been applied frequently to identify components of drought and investigate their statistical properties (Yevjevich 1967; Lee et al., 2017). A Run is a portion of a time series where all the values of indicator are below a specific threshold (Jamro et al., 2020). According to Li et al., (2017), a drought event can be defined as a consecutive sequence of months with a drought index value is below a chosen threshold. In this study, drought onset, termination, duration, severity, intensity and frequency were selected as the drought characteristics to analyze drought over the LRB. Based on the Run Theory the following factors were taken into consideration.

i. **Drought onset (O_D)** is the initiation month of a drought event.

ii. **Drought termination (T_D)** represents the date when the water shortage becomes small enough for the drought to stop persisting.

iii. **Drought duration (D_D)** represents the duration of a drought event, which is the number of months between drought start and its end (Spinoni et al., 2014; Ghosh, 2019). The definition of Drought duration depends on a specific threshold; the drought event starts when the SPEI is continuously negative with the values of SPEI below the threshold. In this study the threshold is set to be -0.5; drought duration starts when the severity is equal to -0.5 or less and its end when the SPEI becomes higher than -0.5.

iv. **Drought Severity (S$_D$)** indicates a cumulative deficiency of a drought parameter below the threshold.

v. **Drought intensity (I$_D$)** refers to the average value of drought parameter below the threshold, which is calculated as the drought severity divided by the duration.

vi. **Drought frequency (F$_D$)** is used to assess drought liability during the study period (Ghosh, 2019). The droughts per 100 years was calculated based on the following equation:

$$F_{D\,j,100} = \frac{Nj}{j.n} * 100(\%)$$

Equation 7

Where, $F_{D\,j,100}$ is the frequency of droughts for a time scale j in 100 years; Nj is the number of months with droughts for time scale j in n-year set; j is time scale (3-, 12-months); n is the number of years in the dataset.

The characteristics of drought events were calculated based on a python-script illustrated on the Appendix 1. The script is based on the Run Theory method and uses a threshold of -0.5 to detect drought over the study area; this means that values of SPEI below -0.5 are considered as areas with drought. The threshold was chosen based on Table 1. The code was developed to calculate the characteristics of drought such as onset, termination, duration, severity, intensity and frequency.

3.3.2. NDVI

In this study, the analysis is based on seasonal and annual data, and it was necessary to compute seasonal and annual NDVI values. Seasonal and annual values of NDVI for each station were averaged from the original monthly MODIS VI NDVI data. To locate NDVI values for each station in the study area, we overlapped NVI time series data and the stations that are in analysis; this was done by taking a monthly time series 1km NDVI values of each pixel where the stations are located. The computation of seasonal NDVI was conducted by calculating the mean NDVI for each season: summer (December, January and February), autumn (March, April and May), winter (June, July and August), and spring (September, October and November). As summer begin in December in the study area, we had to include data of December NDVI of 2000 to compute seasonal NDVI from 2001 ton 2018. To compensate for the gap, the month of December 2018 was then removed from the

analysis. The annual NDVI was calculated by averaging their monthly NDVI values from January to December of each year. The equations were calculated as follows:

$$NDVI_{season} = \frac{\sum_{i=1}^{3} NDVI_{month}}{3} \qquad \text{(Equation 8)}$$

$$NDVI_{year} = \frac{\sum_{i=1}^{12} NDVI_{month}}{12} \qquad \text{(Equation 9)}$$

3.3.3. Trend analysis using Mann-Kendall test

A number of statistical tests exists to assess the significance of trends in time series. However, the non-parametric Mann-Kendall test (MK) is widely used to evaluate trends in hydrological and meteorological time series data (Yue S. et al., 2002). According to Giuseppe et al., (2019) many studies apply the MK test of SPEI time series. It is a non-parametric test, which means it work for all distribution and has the advantage of eliminating the outliers.

The MK tests whether there is a trend in the time series. It is based on two hypotheses; one is the null hypothesis (H_0) that expresses the existence of non-monotonic trend in the series, and the other is the alternative hypothesis (H_A), which expresses that the data follow a monotonic trend, this trend can be positive or negative (Pohlert, 2020).

To perform a Mann-Kendall test, we calculate the difference between the value measured after and all the values measured before, (xj-xi), where j>i. The Mann-Kendall test statistic S (Mann, 1945; Kendall, 1975) is calculated according to:

$$S = \sum_{i=1}^{n-1} \sum_{j=i+1}^{n} sgn(x_j - x_i) \qquad \text{Equation 10}$$

Where n is the number of data points, xi and xj are the data values in time series i and j, respectively, and sgn(xj−xi) is the sign function.

The application of trend is done to a time series X_i that is ranked from i=1,2, 3...n-1 and X_j, which is ranked from j=i+1,2,3...n. Each data point xi is taken as a reference point, which is compared with the rest of the data point xj so that,

$$sgn(x_j - x_i) = \begin{cases} +1, > (x_j - x_i) \\ 0, = (x_j - x_i) \\ -1, < (x_j - x_i) \end{cases} \qquad \text{Equation 11}$$

The test statistic S, is then computed as the sum of the integers. A very high positive value of S is an indicator of an upward trend, and a very low negative value indicates a downward trend; when the absolute value of S is small, no trend is indicated (Khambhammettu, 2005). The variance is computed as

$$Var(S) = \frac{n(n-1)(2n+5)-(\sum_{i=1}^{m} t_i(t_i-1)(2t_i+5)}{18}$$
Equation 12

Where n is the number of data points, m is the number of tied groups (a tied group is a set of sample data with the same value), and t_i is the number of data points in the ith group.

According to Kendall, in cases where the sample size n>10, the normalized test statistic Zs is calculated using equation 13.

$$Z_s = \begin{cases} \frac{S-1}{\left[VAR(S)^{1/2}\right]} & if\ S > 0 \\ 0, & if\ S = 0 \\ \frac{S+1}{\left[VAR(S)^{1/2}\right]} & if\ S < 0 \end{cases}$$
Equation 13

Positive values of Zs indicate increasing trends while negative Zs values indicate decreasing trends. The trend test is based on specific a significance level α. If |Zs| >Zs(1- α/2) then a significant trend is present in the data. Zs(1- $\alpha/2$) correspond the value of p= $\alpha/2$. Based on the 5% significance level as an example, if p value is $\leq \alpha$ =0.05, then the alternative hypothesis is accepted, if the p-value is $\geq \alpha$ then the null hypothesis is accepted, which signifies the absence of trend in the data. The hypothesis test, α =0.05 significance level was used in this study.

The statistical significance trend detected using the MK test can be complemented with Sen's slope estimation to determine the magnitude of the trend. The Sen's slope method is used to evaluate the direction of the trend (Giuseppe et al., 2019). A negative slope values indicates the increase of drought events, while a positive slope indicate the decrease of the event (Bulpitt, 1967).

To analyze MK test significance and the trend from Sen's slope, the R package is used in this research. The SPEI data were used to analyze trends of drought in the LRB over the 100 years. The data were divided into seasonal trends based on 3-month scale and annual trend based on 12-month SPEI dataset.

3.3.4. Correlation analysis between NDVI and drought

To reveal the vegetation response to drought, a correlation analysis between NDVI and SPEI values was performed based on the Pearson coefficient analysis. The Pearson coefficient, which ranges from -1 to +1, is a measure of the strength of the linear relationship between two variables (Zhifang et al., 2019). The value -1 represents the perfect negative relationship, while the value +1 represent perfect

positive linear relationship and zero represent no correlation between the variables. The Pearson correlation coefficient is calculated based on equation 14.

$$R_{x,y} = \frac{\sum_{i=1}^{n}[(x_i - \bar{x}) - (y_i - \bar{y})]}{\sqrt{\sum_{i=1}^{n}(x_i - \bar{x})^2 \sum_{i=1}^{n}(y_i - \bar{y})^2}}$$
<div align="right">Equation 14</div>

Where $R_{x,y}$ is the Pearson correlation coefficients between variable x and y, n is the sample size, and $\bar{x}$ and $\bar{y}$ are the means of the two variables.

The NDVI values corresponding to SPEI were used for the analysis of correlation. Using values of SPEI and NDVI data for the nine stations from 2001 to 2018, it was possible to determine the correlation coefficient at 3- and 12-month time scales. Pearson correlations between NDVI and drought were analyzed using Microsoft Excel in this study, the data were organized into seasonal (seasonal NDVI and seasonal SPEI) and annual data for each variable NDVI and SPEI (annual NDVI and annual SPEI). According to Evans (1996), the strength of the absolute value of r can be described as follow: 0-0.19 – very weak, 0.2-0.39 – weak, 0.4-0.59 – moderate, 0.6-0.79 – strong, 0.8-0.1 – very strong.

4. Results

4.1.　　　　3-Month and 12-Month SPEI Time Series

The time series of the monthly values of SPEI for 3-month and 12-month timescales in the years 1918-2018 is shown in Figure 3 and 4. In total 4 stations were chosen to illustrate how SPEI values change over the time; the stations 1, 3, 5 and 8 located in Mozambique, Zimbabwe, Botswana and South Africa, respectively. Other stations are presented in the Appendix 2. As the timescale changes, drought events also change. For timescale of 3-month (Fig. 3) values of SPEI change frequently into positive (wet condition) and negative values (dry condition), and provide a seasonal picture of drought, thus reflecting short duration meteorological drought. While, for the 12-month timescale (Fig. 4), periods with negative SPEI are less frequent but they have longer duration, representing persistence of hydrological drought in the region. This characteristic is observed for all stations in analysis over the study area. Negative SPEI values represent dry periods and positive SPEI values represent humid periods; the values are represented by red and blue bars, respectively. It is important to mention that drought events are defined based on a specific threshold, in this case only values of SPEI that are less than -0.5 represent areas with drought.
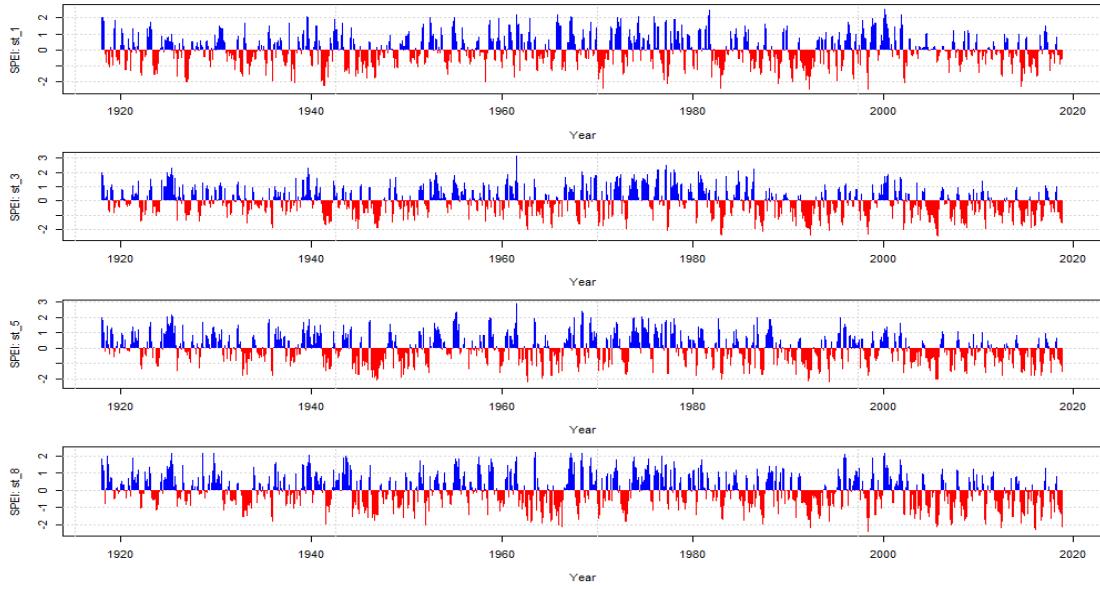
Figure 3. Temporal variability of the SPEI at 3-month-scale from 1918-2018 (stations 1-Mozambique, 3-Zimbawe, 5-Botswana and 8-South Africa, respectively. Positive values (blue bar) of the SPEI represent wet years while the values of the SPEI<-0.5 (red bar) represent years with drought).
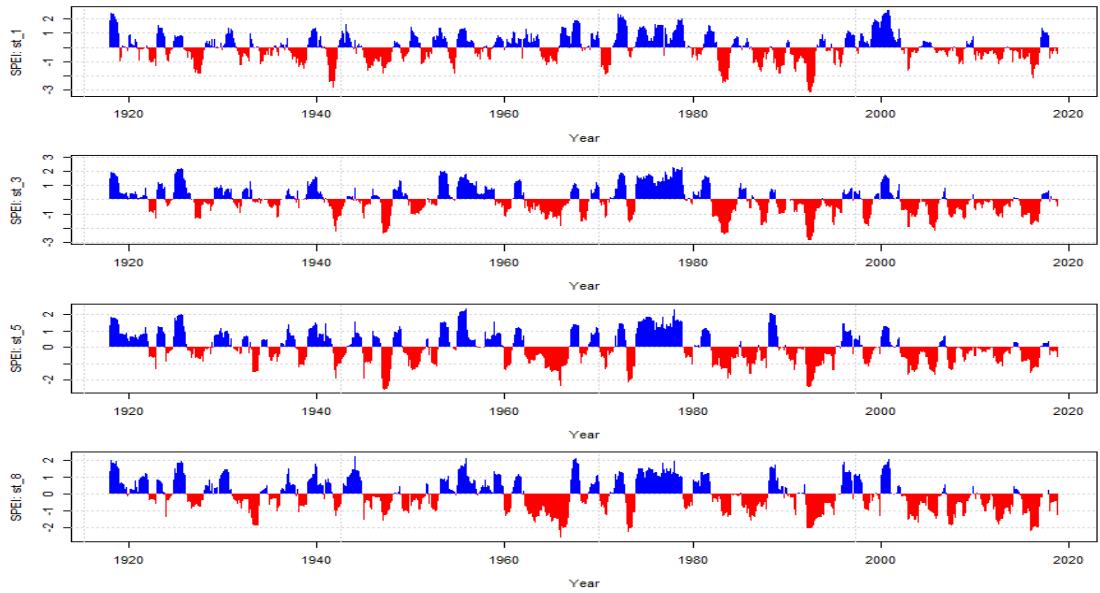
Figure 4. Temporal variability of the SPEI at 12-month-scale from 1918-2018 (stations 1-Mozambique, 3-Zimbawe, 5-Botswana and 8-South Africa, respectively). Positive values (blue bar) of the SPEI represent wet years while the values of the SPEI<-0.5 (red bar) represent years with drought).

4.2.   Onset and termination of drought

The analysis of the beginning and end of the drought is based on seasonality, which means that the beginning and end of the drought is attributed as a sequence of seasons such as summer, autumn, winter and spring. The frequency of drought events that begin or end in each season based on the SPEI 3-month time scale is shown in Fig. 5. The frequency of drought allow the possibility of counting the number of

22

drought events that started or ended in each season. The results reveal that onset and termination of drought occurred in a different time period in the LRB. For stations 1, 3, 5, 7 and 8, the drought does not have a specific season to start; there is no significant difference between the number of times the drought starts for each season. On the other hand, stations 2 and 6 have a tendency to start during winter, while stations 4 and 9 have a tendency to start during spring; this can be seen in the graph in Fig. 7(a). The drought termination, on the other hand, seems to have an inclination for the season between spring and autumn for the majority of the stations. In the western, lower lands (stations 1, 2, 3 and 7) spring is the major season for the end of drought, while the stations 3, 4, 5, 8 and 9 demise of drought is during autumn, and station 6 in the winter.
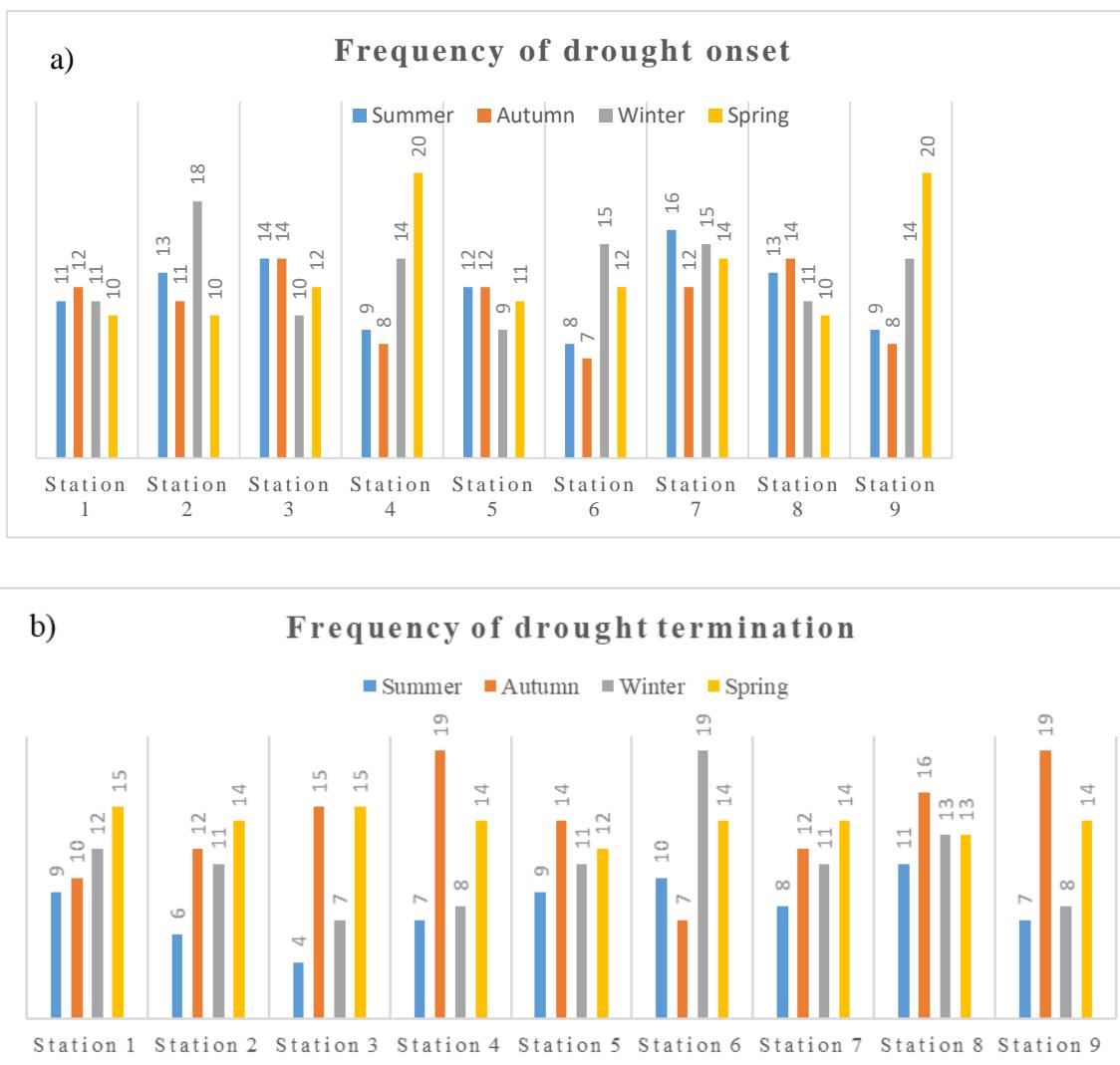
Figure 5. Frequency of drought events. Drought onset (a) and drought termination (b) were calculated based on the different seasons: Summer (DJF), Autumn (MAM), Winter (JJA) and Spring (SON) in the Limpopo River Basin.

4.3. Duration of drought events

Table 2 illustrates the three longest drought events in the LRB for all stations under analysis. The annual and seasonal drought duration over the LRB varied significantly from 1918 to 2018. Based on the 3-month time scale, several droughts were identified in the basin. We decided to illustrate only the three longest droughts for each meteorological stations over the study area. The analysis revealed the following droughts: 1941 to 1942, 1945, 1946 to 1947, 1965 to 1966, 1970, 1972 to 1973, 1986 to 1987, 1991 to 1992, 1994 to 1995, 2004 to 2005, 2006 to 2007 and 2011 to 2012 droughts. The longest drought lasted 17 months during August 2004 to December 2005, and the meteorological stations that registered this drought were stations 3 and 7, located in Zimbabwe and South Africa, respectively. The subsequent droughts that had the longest duration were the droughts from 1946 to 1947, 1991 to 1992 and 2004 to 2005 all with a duration of 16 months; the values were registered for the stations 5, 2, 4 and 7.

Based on the 12-month time scale, the following years presented droughts with longer durations: 1945-1946, 1950-1951, 1962-1966, 1963-1966, 1982-1984, 1990-1993, 1992-1994, 2002-2004, 2012-2014, 2004-2016, 2014-2017, 2015-2016. The longest droughts were registered at the stations 7, 8 and 6 with the following durations: 59, 58 and 45 months from 1962 to 1966 for stations 7 and 8; and from 1983-1986 for station 6. Station 1 has the shortest drought duration for the top three droughts in analysis over the LRB.

4.4. Drought Severity and Intensity

We identified the top three severe and intense droughts over the study area. For all the stations in analysis based on the 3-month timescale (Table 3), the following years can be considered as severely dry: 1941-1942, 1946-1947, 1970, 1972-1973, 1986-1987, 1991-1992, 2004-2005, 2011-2012 and 2013. The most severe drought registered for all the stations based on 3-month scale was registered in station 2, located in Mozambique with a value of 26.67 occurred in 1991 to 1992, followed by the stations 5 and 7 with values of 24.94 for both of the stations occurred in 1946-1947 and 1991-1992 respectively. The highest intensities (Table 4) were recorded at stations 6, 1, 9 and 8 with the following values 2.01, 2.0, 1.96 and 1.95, respectively, and were registered in the following years: 1937 for station 1 and 2005 for stations 6, 8 and 9.

The 12-month time scale suggest that the most severe drought (Table 3) occurred at the station 8 in South Africa having a value of 79.75 during 1962-1963, followed by the station 6 during 1983-1986, station 7 during 1962-1963 and station 2 during 1982-1984 with the following severity values 66.36, 63.29 and 52.85 in Botswana, South Africa and Mozambique respectively. The most intense drought based on the 12-month time scale (Table 4) was registered in the station 2, with a value of 2.23, followed by the stations 5, 1 and 3 having the following intensity 2.07, 1.98 and 1.97. The following years were the most intense years with droughts, 1982 to 1983, 1991 to 1993, 1947 to 1948 for stations 3, 4 and 5, 2007 to 2008 station 6, 1946 to 1948 for station 7 and 1992 to 1993 for station 9.

Table 2. The three longest droughts in the Limpopo River Basin occurred between 1918 and 2018

Countries	lag-time	St.	Onset	Termination	D_D (m)	S_D	Onset	Termination	D_D (m)	S_D	Onset	Termination	D_D (m)	S_D
							3 most long Drought for each station							
Mozambique	3-month	1	7/16/1991	7/16/1992	13	20.27	1/16/1970	12/16/1970	12	14.80	4/16/1945	12/16/1945	9	9.88
		2	8/16/1991	11/16/1992	16	26.67	10/16/2004	12/16/2005	15	21.80	7/16/1986	7/16/1987	13	18.86
Zimbabwe		3	8/16/2004	12/16/2005	17	23.86	6/16/1991	7/16/1992	14	21.91	3/16/1941	2/15/1942	12	15.71
		4	8/16/2004	11/16/2005	16	21.86	5/16/1946	8/16/1947	16	20.00	6/16/1991	7/16/1992	14	19.04
Botswana		5	5/16/1946	8/16/1947	16	24.94	6/16/1991	7/16/1992	14	19.36	8/16/1972	5/16/1973	10	12.30
		6	9/16/2011	8/16/2012	12	13.52	9/16/2006	8/16/2007	12	17.98	9/16/2011	8/16/2012	12	13.52
South Africa		7	8/16/2004	12/16/2005	17	21.11	8/16/1991	11/16/1992	16	24.94	2/15/1941	2/15/1942	13	16.65
		8	6/16/1991	7/16/1992	14	17.79	7/16/1965	6/16/1966	12	14.88	6/16/1972	5/16/1973	12	15.31
		9	9/16/2011	8/16/2012	12	17.79	9/16/1965	8/16/1966	12	13.43	5/16/1994	3/16/1995	11	12.89
Mozambique	12-month	1	10/16/1990	2/15/1993	29	49.45	2/15/1945	11/16/1946	22	24.27	2/15/1964	8/16/1965	19	18.34
		2	2/15/1982	10/16/1984	33	52.85	11/16/1963	2/15/1966	28	32.64	1/16/1950	8/16/1951	20	18.01
Zimbabwe		3	2/15/1982	9/16/1984	32	48.02	11/16/1963	5/16/1966	31	34.59	1/16/2015	12/16/2016	24	32.28
		4	2/15/1982	12/16/1984	35	47.27	12/16/1963	2/15/1966	27	34.34	1/16/2015	12/16/2016	24	34.29
Botswana		5	3/16/1964	11/16/1966	33	43.85	1/16/1992	1/16/1994	25	39.79	3/16/2002	2/15/2004	24	26.89
		6	2/15/1983	10/16/1986	45	66.36	12/16/1963	9/16/1966	34	37.96	12/16/2014	12/16/2016	25	39.36
South Africa		7	2/15/1962	12/16/1966	59	63.29	2/15/1982	9/16/1984	32	50.82	1/16/1992	10/16/1993	22	38.50
		8	3/16/1962	12/16/1966	58	79.75	1/16/1992	6/16/1994	30	41.63	1/16/2012	1/16/2014	25	28.78
		9	1/16/2012	10/16/2014	34	50.13	12/16/2014	1/16/2017	26	38.58	11/16/2002	11/16/2004	25	25.76

Table 3. The three most severe droughts for each station in the Limpopo River Basin occurred between 1918 and 2018

			3 most Severe Drought for each station											
Countries	lag-time	St.	Onset	Termination	D_D (m)	S_D	Onset	Termination	D_D	S_D	Onset	Termination	D_D	S_D
Mozambique	3-month	1	7/16/1991	7/16/1992	13	20.27	1/16/1970	12/16/1970	12	14.80	1/16/1941	7/16/1941	7	12.47
		2	8/16/1991	11/16/1992	16	26.67	10/16/2004	12/16/2005	15	21.80	7/16/1986	7/16/1987	13	18.86
Zimbabwe		3	8/16/2004	12/16/2005	17	23.86	6/16/1991	7/16/1992	14	21.91	3/16/1941	2/15/1942	12	15.71
		4	8/16/2004	11/16/2005	16	21.86	5/16/1946	8/16/1947	16	20.00	6/16/1991	7/16/1992	14	19.04
Botswana		5	5/16/1946	8/16/1947	16	24.94	6/16/1991	7/16/1992	14	19.36	8/16/1972	5/16/1973	10	12.30
		6	9/16/2006	8/16/2007	12	17.98	9/16/2011	8/16/2012	12	13.52	9/16/2011	8/16/2012	12	13.52
South Africa		7	8/16/1991	11/16/1992	16	24.94	8/16/2004	12/16/2005	17	21.11	5/16/1946	4/16/1947	12	17.20
		8	6/16/1991	7/16/1992	14	17.79	6/16/1972	5/16/1973	12	15.31	7/16/1965	6/16/1966	12	14.88
		9	9/16/2011	8/16/2012	12	17.79	11/16/1991	7/16/1992	9	17.41	2/15/2013	11/16/2013	10	15.32
Mozambique	12-month	1	10/16/1990	2/15/1993	29	49.45	9/16/1982	12/16/1983	16	31.62	3/16/1941	4/16/1942	14	26.07
		2	2/15/1982	10/16/1984	33	52.85	9/16/1991	2/15/1993	18	40.10	11/16/1963	2/15/1966	28	32.64
Zimbabwe		3	2/15/1982	9/16/1984	32	48.02	12/16/1991	8/16/1993	21	37.29	11/16/1963	5/16/1966	31	34.59
		4	2/15/1982	12/16/1984	35	47.27	12/16/1963	2/15/1966	27	34.34	1/16/2015	12/16/2016	24	34.29
Botswana		5	1/16/1992	4/16/1995	40	49.20	2/15/2002	2/15/2006	49	48.82	11/16/1963	11/16/1966	37	45.62
		6	2/15/1983	10/16/1986	45	66.36	1/16/1992	12/16/1993	24	40.19	12/16/2014	12/16/2016	25	39.36
South Africa		7	2/15/1962	12/16/1966	59	63.29	2/15/1982	9/16/1984	32	50.82	1/16/1992	10/16/1993	22	38.50
		8	3/16/1962	12/16/1966	58	79.75	1/16/1992	6/16/1994	30	41.63	2/15/2015	12/16/2016	23	35.31
		9	1/16/2012	10/16/2014	34	50.13	12/16/2014	1/16/2017	26	38.58	1/16/1992	9/16/1993	21	38.31

Table 4. The three most intense droughts for each station in the Limpopo River Basin occurred between 1918 and 2018.

Countries	lag-time	St.	Onset	Termination	D_D (m)	I_D	Onset	Termination	D_D (m)	I_D	Onset	Termination	D_D (m)	I_D
											3 most Intense Drought for each station			
Mozambique	3-month	1	12/16/1937	12/16/1937	1	2.00	1/16/1941	7/16/1941	7	1.78	4/16/1998	7/16/1998	4	1.62
		2	6/16/1977	7/16/1977	2	1.73	10/16/1982	6/16/1983	9	1.72	8/16/1991	11/16/1992	16	1.67
Zimbabwe		3	12/16/1982	6/16/1983	7	1.73	7/16/1962	10/16/1962	4	1.62	6/16/1991	7/16/1992	14	1.56
		4	6/16/1977	7/16/1977	2	1.81	7/16/1962	10/16/1962	4	1.79	7/16/2015	2/15/2016	8	1.79
Botswana		5	12/16/1944	2/15/1945	3	1.76	6/16/1977	7/16/1977	2	1.71	7/16/1962	10/16/1962	4	1.69
		6	7/16/2005	12/16/2005	6	2.01	12/16/1944	2/15/1945	3	1.94	9/16/2011	8/16/2012	12	1.91
South Africa		7	7/16/2013	9/16/2013	3	1.74	10/16/1982	6/16/1983	9	1.63	2/15/2002	5/16/2002	4	1.60
		8	7/16/2005	12/16/2005	6	1.95	2/15/1963	4/16/1963	3	1.80	4/16/1998	8/16/1998	5	1.76
		9	7/16/2005	12/16/2005	6	1.96	11/16/1991	7/16/1992	9	1.93	4/16/1998	8/16/1998	5	1.80
Mozambique	12-month	1	9/16/1982	12/16/1983	16	1.98	3/16/1941	4/16/1942	14	1.86	10/16/1990	2/15/1993	29	1.71
		2	9/16/1991	2/15/1993	18	2.23	12/16/1946	1/16/1948	14	2.03	1/16/2005	2/15/2006	14	1.61
Zimbabwe		3	1/16/1947	1/16/1948	13	1.97	12/16/1991	8/16/1993	21	1.92	1/16/2005	2/15/2006	14	1.64
		4	1/16/1947	1/16/1948	13	1.92	2/15/1992	1/16/1993	12	1.69	1/16/2005	2/15/2006	14	1.44
Botswana		5	1/16/1947	2/15/1948	14	2.07	1/16/1973	11/16/1973	11	1.73	11/16/1963	11/16/1966	37	1.23
		6	1/16/2007	2/15/2008	14	1.86	1/16/1992	12/16/1993	24	1.67	12/16/2014	12/16/2016	25	1.57
South Africa		7	12/16/1946	1/16/1948	14	1.85	1/16/1992	10/16/1993	22	1.75	2/15/1982	9/16/1984	32	1.59
		8	12/16/1972	11/16/1973	12	1.69	2/15/2015	12/16/2016	23	1.54	11/16/1932	12/16/1933	14	1.48
		9	1/16/1992	9/16/1993	21	1.82	2/15/2007	1/16/2008	12	1.64	10/16/1965	12/16/1966	15	1.53

Where: D_D (m) – Drought duration in months; S_D – Drought severity; I_D – Drought intensity

4.5.   Drought frequency

Figure 6 illustrates the drought frequency at 9 meteorological stations in the LRB based on 3- and 12-month time scales. The results show that mild droughts occur most frequently, followed by moderate, severe and extreme drought, with less frequency. At 3-month time scale, all the stations located in South Africa and the station 1 located in the lower Limpopo in Mozambique experienced higher occurrence of mild drought, with values between 67 and 70 droughts in 100 years with a duration of 3 months. Moderate drought had high frequency in two countries Mozambique (station 1) and Botswana (station 6); the number of droughts varies between 50 and 53 droughts lasting 3 months. Severe drought had high occurrence of droughts with a duration of 3 months spread along the three countries of the basin except the stations located in Mozambique; the number of droughts vary between 26 and 28 droughts in 100 years. Extreme drought on the other hand occur with high frequency in the stations 2 and 6 located in the west arid zone of Mozambique and Botswana respectively, with the number of 9 and 8 droughts in 100 year. Whereas, for a drought with duration of 12-months mild drought occur in all the stations of South Africa and in the west part of Mozambique in the basin. The numbers of drought with a duration of 12 months are: 17 for stations 7 and 8 both in South Africa, and 18 for station 2 and 9 in Mozambique and South Africa, respectively, during the 100 years in analysis. Whereas, extreme drought occurred with high frequency at the stations located in Mozambique and one station in Zimbabwe, both with a value of 3 droughts in the time period of the analysis. The station 2 located in the arid zone of Mozambique is highly prone to extreme drought both for 3- and 12 month SPEI time scale.

4.6.   Spatial extent of the most severe drought

The spatial analysis on drought characteristics is a crucial procedure for understanding droughts (Fung et al., 2020). Figure 7 illustrate the most severe drought during the period of 1918 to 2018 over the LRB. The drought that severely affected the basin was the 1991-1992 drought, the east and central part of the basin were extremely affected, with 77% of the stations affected and the west part of the basin was severely affected. Another drought that severely affected the basin was the 1946-1947 drought, the north part of the basin was extremely affected by this drought with the northeast part severely affected. Followed by the 2015-2016 large area of the basin was also severely affected. Those are some examples of the spatial extent of

drought that affected the basin during the period of analysis. Droughts affected different regions of the basin differently. In addition, depending on the year there are some areas that were more affected than others.
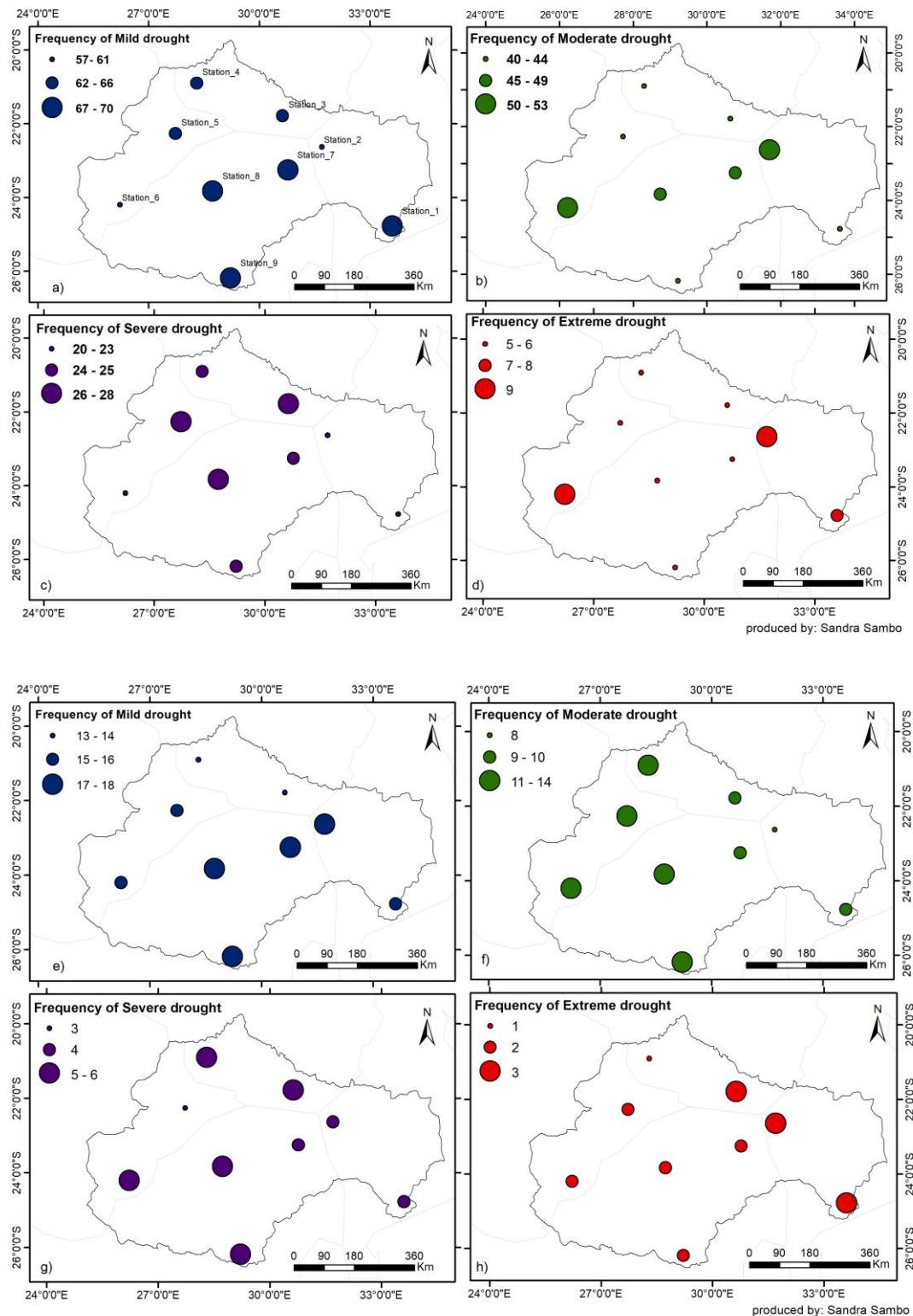

Figure 6. Frequency of drought in the Limpopo River Basin based on the different degree of severity (Mild (a, e), Moderate (b, f), severe (c, g) and extreme drought (d, h)) based on 3-month (a, b, c and d) and 12-month (e, f, g and h) SPEI.
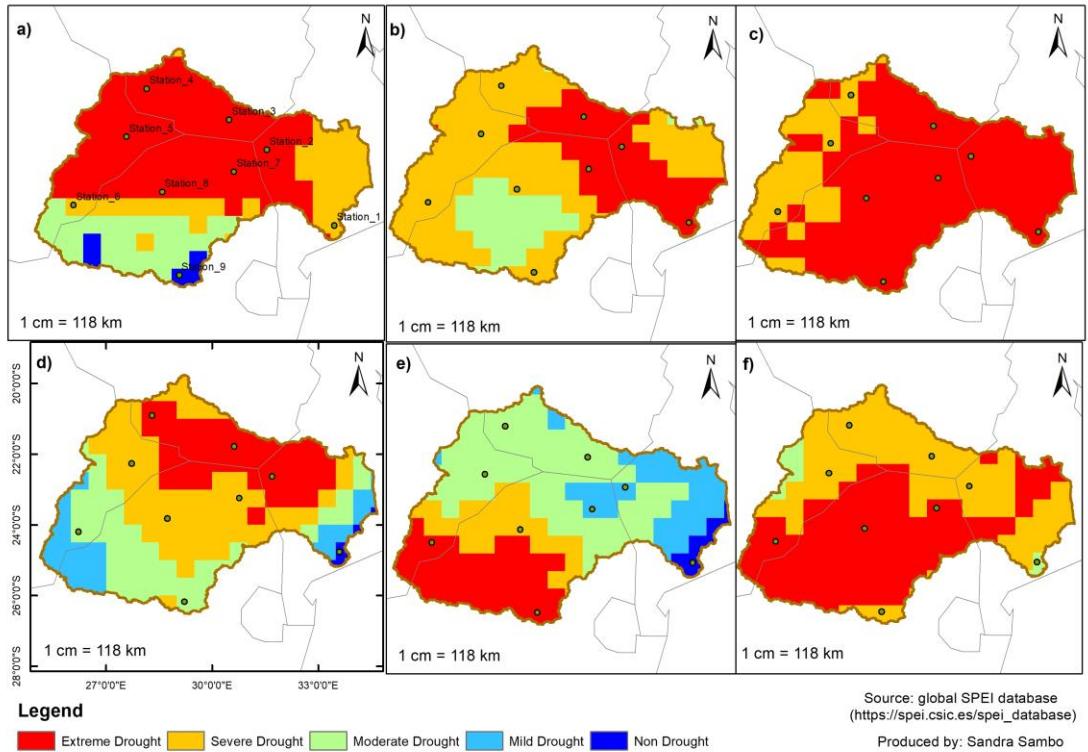
Figure 7. Spatial extent of one of the most severe droughts indicated by 12 month SPEI. Some of the most severe droughts were registered in the years: 1946-1947 (a), 1982-1983 (b), 1991-1992 (c), 2004-2005 (d), 2006-2007 (e) and 2015-2016 (f). Data was used from a global dataset of SPEI.

4.7. Trend analysis of SPEI series

The identification of statically significant trends in SPEI with the objective of studying the evolution of the characteristics of drought from 1918 to 2018 has been carried out using the non-parametric Mann-Kendall trend test and Sen's slope. Using the R program, it was possible to identify the following parameters: The Zs value, p-value and Sen's slope; these values were used for the analysis of trend in the data. Zs values are used to analyze if there is an increase or decrease of trend in the data, while the p-value was used to analyze the significance of the trend. In order to analyze the magnitude of the trend, the Sen's slope value is used. The results of these parameters are described in the Appendix 3; the values were then used to produce the map in Fig. 8 and the graph in Fig. 9. For the analysis of drought, a positive trend indicates the intensification of wet conditions and a negative trend indicates the amplification of dry conditions.

Figure 8 shows the annual and seasonal distribution of temporal trends of SPEI characterized by the test statistic Zs values at 9 meteorological stations; blue triangles

represent an insignificant increase trend, while red small triangle represents a decrease trend, but not at a significant p-value < 0.05. Large red triangles indicate increasing significant trends at the 95% confidence level. Based on the p-value, it was possible to find stations where trends show a significant change over the 100 years. The 12-month time scale SPEI exhibited a significant decrease trend for most stations in the basin; the results show that for the annual SPEI 89% of the stations got a drier significant trend with only one station showing slight dry trends.

The four seasonal trends were also analyzed in the study, by SPEI 3-months. The trend along the last century is that the LRB is getting drier along the years, especially the winters, except for station 1 located in Mozambique that experienced a slight dry trends. For stations 6 located in Botswana and station 8 located in South Africa, also the autumn and spring seasons are getting drier.
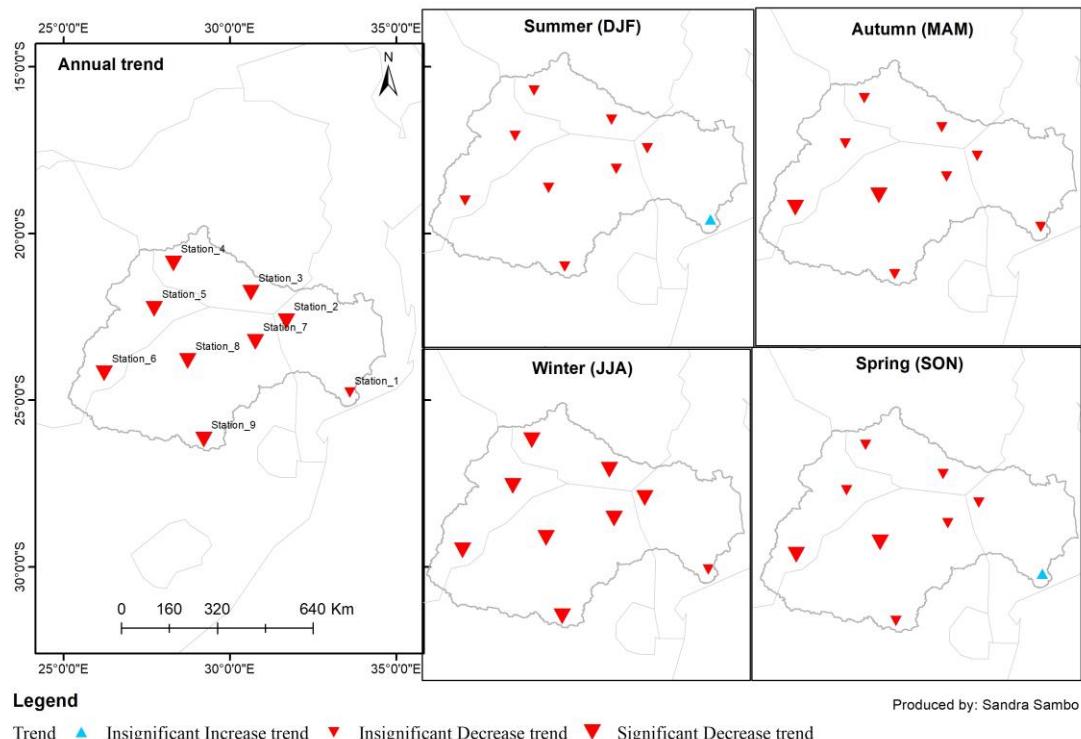
Figure 8. Annual and seasonal trends at 9 meteorological stations over the LRB for the period 1918-2018. Positive trends (blue triangle) indicate an increase in the wet condition while negative trends (red triangles) indicate an increase in the dry condition.

The Sen's slope (Figure 9) was used to estimate the slope of the trend (change per unit time) in the data. According to the results of Sen's slope for the period of study the average tendency of the annual SPEI decreases significantly by -0.009/year in 89% of the stations in the LRB, and the remaining 11%, which is represented by

station 1, indicate an insignificant decrease of the trend by -0.002/year. The variation of each annual magnitude of trend for each station is shown in Figure 11. The magnitude of trends in annual SPEI vary between -0.002/year and -0.009/year for the 100 year study period, with the lowest value in the station 1 located in the lower Limpopo and the highest magnitude in the station 3 in Zimbabwe.

The four seasons also experienced a decrease of trend in the LRB, with the average most significant trend of -0.011/year in winter, where eight stations showed a significant decrease trend and station one showed an insignificant decrease trend, the magnitude of trends in winter vary between -0.003/year and -0.016/year. In autumn 77.8% of the stations indicates an insignificant decrease trend with the average of -0.006/year, while 22.2% indicates a significant decrease trend with a magnitude of -0.008/y and -0.009/y for stations 6 and 8, respectively. Summer also experienced an insignificant decrease trend for 89% of the stations with the station one indicating an insignificant increase trend by 0.003/year. Spring registered an insignificant trend for 6 station, 2 stations (6 and 8) experienced a significant decrease trend and 1 station (station 1) experienced a slight increase trend. For all the stations the Sen's slope agrees with the Mann-Kendall Statistic, where the MK statistic indicates an increase or decrease trend the Sen's slope also indicate the same direction of trend.
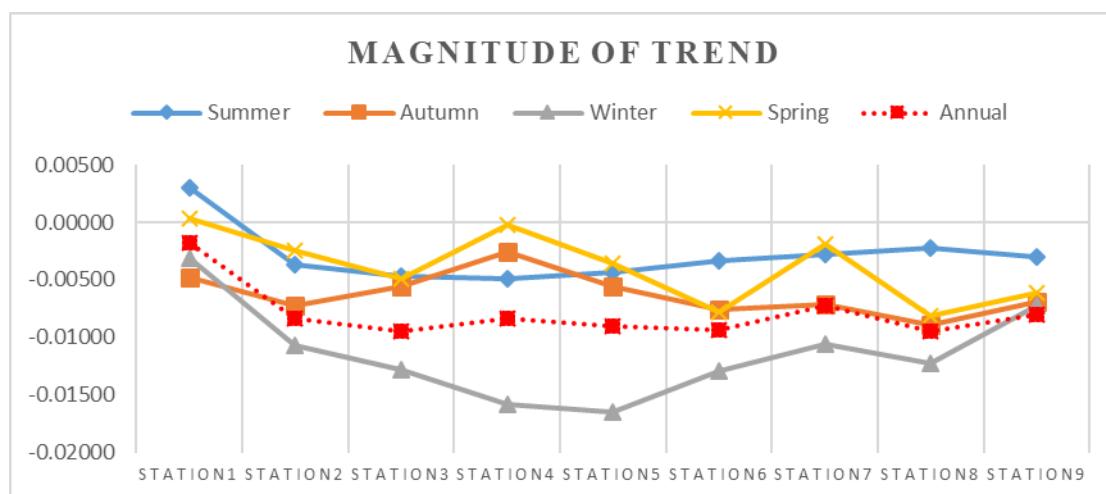
Figure 9. Magnitude of trend based on the Sen's slope value over the study area. The values indicate the change of SPEI per year during 1918 to 2018. The analyze is based on the seasonal and annual SPEI values.

4.8.   Response of vegetation to drought

In order to analyze the response of vegetation to drought, correlation between NDVI and drought was performed using Pearson correlation analysis. For each station, correlation analyses were conducted between the seasonal and annual

timescales of the SPEI and NDVI. Figure 10 shows the scatterplots of NDVI and the 3- and 12-month SPEI.

At the seasonal time scale, the majority of the scatterplots show that the correlation between the two variables is strongest around autumn and spring. Therefore, there is no clear pattern about correlation between seasonal NDVI and SPEI in the study area. It is possible to see a weak correlation between seasonal NDVI and SPEI for 33% of the stations (stations 3, 5 and 9 with r<0.4) in spring; for autumn all the stations have shown a strong correlation between seasonal SPEI and NDVI with 100% of the stations having r>0.4. The correlation between NDVI and SPEI were generally low during winter and summer. By analyzing winter 78% of the stations have a correlation coefficient less than 0.4; during winter the correlation is weak between the two variables (r=0.21) on average. For summer, 44% of the stations have a correlation coefficient less than 0.4; seasonal SPEI and NDVI have an average correlation (r=0.32). The strongest correlation between seasonal NDVI and SPEI was found in spring, registered for the station 6, with r=0.7. Autumn also registered a high correlation values for the stations 2, 3, 4 and 7, with r >0.6. Autumn and spring have a higher average correlation (r=0.55 and r=0.44, respectively).

Figure 10 shows that for most of the stations the annual correlation between the two variables suggest a high positive correlation with 89% of the stations having r>0.4. The 12-month timescale has an average correlation coefficient of 0.59.

In Figure 10, only scatterplots for stations 1, 3, 5 and 8 are illustrated; other scatterplots are illustrated in the Appendix 6.
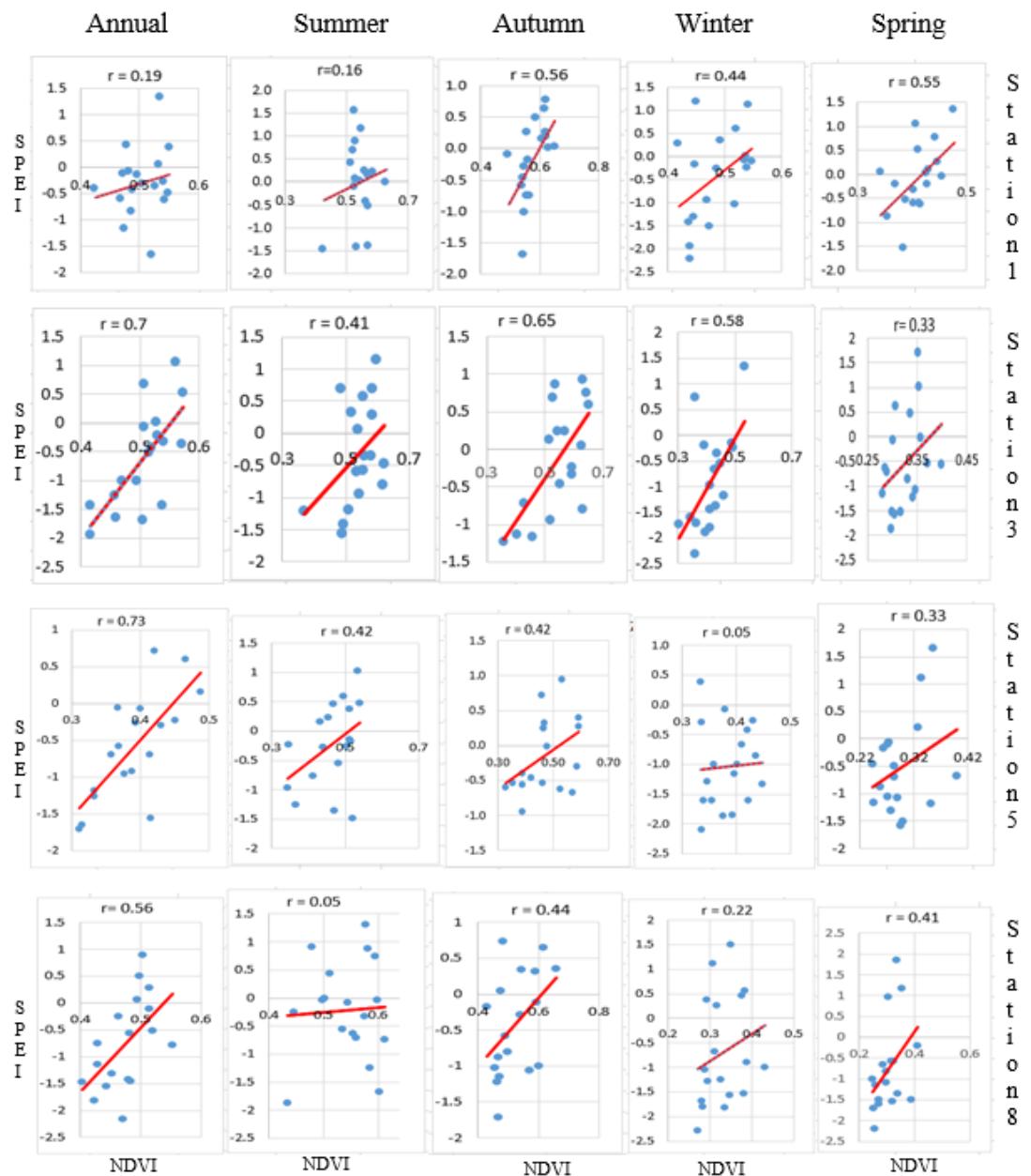
Figure 10. Seasonal and annual correlation coefficient (r) between NDVI and SPEI. Each dot represents one year between 2001 and 2018.

5. Discussion

The Standardized Precipitation Evapotranspiration Index (SPEI) has been widely used in diverse studies that analyze drought characteristics (Jin et al., 2019; Fung et al., 2020), drought atmosphere mechanism (Manzano et al., 2019), drought monitoring and analysis (Tirivarombo et al., 2018; Abbasin et al., 2019) and climate change (Mehr et al., 2020). According to Begueria et al. (2014), several drought studies that used SPEI to detect drought characteristics reported that SPEI correlated better with ecological and hydrological variables than other drought indices. In this study, an effort has been made to determine the characteristics of drought such as onset, termination, duration, severity, intensity and frequency over the Limpopo River Basin based on SPEI from 1918 to 2018.

The understanding obtained through detailed historical analysis of drought events offer possibilities to realize better drought management and planning to mitigate impacts of droughts (Vicente-Serrano et al., 2012); in addition, the analysis of historical droughts can provide information on water demand deficits, which is essential for drought risk reduction (Masih et al., 2014). Previous droughts events can facilitate improved drought mitigation and preparations plans. In addition this can help to determine the spatial and temporal variability of drought risk and the vulnerability of water resources, vegetation systems and drought society (Mishra and Singh, 2010).

Although the SPEI dataset used in this study was extracted from a database that has a low spatial resolution, previous studies show that the SPEI data used in this study can truly be used to analyze characteristics of drought in Africa, especially in the Limpopo River Basin. Taking as an example, the study of Peng et al., (2020), which compared the widely used coarse-resolution global SPEI data and the high spatial resolution (5 km) SPEI data to investigate its capability for drought detection in Africa. The researcher concluded that both SPEI with coarse and high spatial resolution dataset performed well the characterization of droughts events and are well correlated with NDVI. Not to mention that for our case study, the index was able to detect all droughts that were detected in previous studies.

For further studies, it would be good to include the land cover, elevation, temperature and precipitation component as input data to observe the correlation between these parameters and the drought index; this would help to better interpret the results obtained in this study. It would help us to understand whether droughts

tend to increase due to the increase in temperature and the decrease in precipitation or just one factor puts greater pressure on the basin to the point where recurring drought frequencies occur. The land cover map will help to understand how different types of vegetation respond to drought.

5.1. Onset and Termination of droughts in Limpopo River Basin

The initiation and cessation are the two most crucial issues associated with monitoring and assessing drought (Shah and Mirsha, 2020). The beginning and end of a drought are difficult to determine, since the effects of drought often accumulate slowly over a considerable period of time and can last for years after the event has ended (Whilhite, 1993). In addition, the drought may end abruptly after some heavy rainfall (Mo, 2011). However, based on the drought index SPEI and the Run Theory method, it was possible in this study to determine the characteristics of drought as described above. Based on the results of the Run Theory method, it was possible to identify the onset and termination of droughts during 1918 to 2018 in each station. Having the results of onset and termination of droughts for both 3- and 12-month time scale, the results of seasonal SPEI (SPEI3) was then used to compute the seasonal frequency of drought, in order to analyze if droughts have a general time to begin or demise according to the different seasons (summer, autumn, winter and spring) in the LRB. The frequency of the beginning and end of the drought was used to determine the season that has the highest occurrence of beginning or end of drought; in addition, it was possible to see how the frequency varies for the different meteorological stations in the study area.

The results of frequency of drought suggest that the number of droughts onsets and terminations vary by the region. This can be due to the fact that precipitation and temperature also varies by region and these factors plays a role in determining the preferred season for onset and drought termination (Mo, 2011). For the majority of the stations (1, 3, 5, 7 and 8) located in the east, central and north part of the basin, the onset of drought did not show any pattern; this implies that in the basin drought can start in any time of the year. On the other hand, drought termination seems to show a pattern about a preferable time for a drought to end; for the majority of the stations drought terminates during autumn and spring (in the western stations). This implies that drought that terminates during spring (September, October and November) is linked to the rainfall season that usually begins in early summer (late October to early

December); this finding applies to all the stations located in the eastern part of the basin (stations 1, 2, 3 and 7). For stations located in the north and south part of the basin, the drought has a higher tendency to terminate during autumn (March, April and May); this can be linked to the rainfall period that occur during March and early April in the Basin.

According to Shah and Mirsha (2020) the analysis of the beginning and end of drought for the identified stations can be beneficial to the drought management community and policy makers. In addition, the knowledge of drought onset is crucial, as it can improve a better understating of the conditions associated with drought and can be useful for the improvement of the drought early warm system (Mo., 2011). In the Limpopo River Basin, the results show that drought termination can be more easy to predict than drought onset. As the drought termination has a preferred season to cease during autumn and spring for the majority of the stations in the Limpopo River Basin.

5.2. Frequency of drought in the Limpopo River Basin

According to Masih et al., (2014) drought became more frequent during the last 50 years in Africa; in addition, most of Africa has suffered severe droughts in the past decades. According to Masih et al. (2014) the semi-arid and sub-humid regions of Africa are the most drought prone regions. This is due to the climate variability in these countries and also due to other reasons such as poverty, high dependence on rain-fed agriculture and poor infrastructure to manage resources and recover from disasters. To analyze the numbers of drought events that occurred in the LRB during 100 years, the frequency of drought based on the different degrees of severity (mild, moderate, severe and extreme) was investigated in this study. Understanding the frequency of drought is important for crop production and this can be done based on SPEI index with short duration (eg. SPEI3). According to the results, the frequency of droughts increases for short-term period (3-mont SPEI); when the timescale increases (12-month-SPEI) the frequency of drought events decreases. The SPEI for 3- and 12-month time scales gives the opportunity to illustrate the relationship between the number of months with droughts based on different drought severity. Mild drought is more frequent for all the stations over the basin for both 3– and 12-month time scale. Considering the sum of the different degrees of severity of the drought, the country that experienced the highest occurrence of droughts based on the 3-month and 12-

month time scale in the period between 1918 and 2018 was South Africa, with a total of 148 number of droughts lasting 3 months and 37 droughts lasting 12 months. The lowest number of droughts was registered in the lower Limpopo Basin in Mozambique with a total of 137 and 32 drought events with durations of 3 months and 12 months, respectively. The droughts in the Limpopo River Basin occurred in different periods for the different regions of the basin, so there were droughts that affected the whole basin and others that affected only a part of it. For that reason, the different degrees of drought severity affected parts of the basin differently. According to the results of summing drought severity, the southern part of the basin is more prone to drought with a duration of 3 months.

The results of drought frequency obtained using the 3- and 12-month SPEI, give a very valuable characteristic that is descriptive of the local climate in the LRB. Many studies (Gebre and Getahum, 2016) assume that drought has occurred very frequently in the region, but only SPEI gives the opportunity to illustrate the relationship between the number of months with drought for different timescales (Łabedzki, 2007).

The fact that South Africa is more prone to drought than other areas of the basin does not mean that the impact of drought is greater in this region. The vulnerability to drought varies per country; for example, the economic impact of the 1991-1992 drought was much higher in Mozambique and Zimbabwe compared to South Africa and Botswana (Masih et al, 2014). For that reason further analysis about severity, intensity and duration of drought are also analyzed in this study to analyze how drought severity affected the region. In addition, Todisco et al., (2012) related that frequency of drought occurrence is not adequate for drought evaluation; this should be related to other factors such as severity and duration of droughts.

5.3. The most severe droughts that affected the Limpopo River Basin

Intensive drought events were observed on a large scale for all continents in recent decades and severely affected large areas around the world (Mirsha and Singh, 2010). In the past decades, LRB, too, has experienced serious drought, which has led to crop failures, high economic losses and the need for humanitarian aid (Trambauer et al., 2015). To determine the most severe drought that affected the LRB region we performed an analysis of the drought duration, severity and intensity for the different stations in the LRB. According to FAO (2004) a series of consecutive drought events

or severe drought events can be a triggering agent for disaster that exacerbates social and economic problems, and reduce the overall security of society's livelihood. These problems are more critical where economies are less diverse and practically all depend directly or indirectly on agriculture. The duration of drought was analyzed in this study in order to understand the characteristic of drought duration over the study area, in addition to analyze if there is a correlation between drought duration, severity and intensity of drought. The duration of drought is not only important for understanding the characteristics of drought over the study area, but is useful for rainfed crop production as it can be linked to growing period (Makondo and Thomas, 2020). Short and long-term drought conditions affect crop growth. The 3-month time scale drought was used in this study to study the characteristic of drought duration that may affect agricultural drought. This type of drought may affect crop growth, resulting in a crop failure, especially when it coincides with the growing season between October to March (spring and summer) in the LRB. According to McNutt (2014) the consequence of continued drought can be far-reaching, affecting food security and even global economy. In addition, prolonged periods of abnormally high drought in the areas depending on agriculture such the majority part of the Limpopo river basin drought can have devastating effects on already marginal levels of productions endangering subsistence agriculture (FAO, 2004).

The three worst drought events were selected based on the duration, severity and intensity of drought in the nine stations under study. For all the stations there are similarities between drought severity and duration. The longest drought had also the highest severity for most of the stations. On the other hand, not every station that had higher severity had the highest intensity. The years that recorded the higher intensity, duration and severity of drought for 3-months and 12-months timescale registered in different stations were 1941-1942, 1946-1947, 1947-1948, 1963, 1972-1973, 1982-1983, 1990-1993, 2005-2006, 2015-2016. The drought intensity, severity and duration were used to find the worst droughts that affected the basin. The results show that the 1946-1947, 1982-1983, 1991-1992, 2004-2005, 2006-2007 and 2015-2016 were the worst droughts that occurred in Limpopo River Basin, which affected most of the stations; some of them affected the whole region while other affected only part of it. These drought events were also identified in previous studies (Masih 2014; Gebre and Getahum, 2016; Lindevall, 2016).

The identified severe droughts were similar as found in a study of Lindevall (2016), who analyzed disaster risk and vulnerability of drought and floods over the Limpopo river basin. All results of droughts found in this study are similar to the results of Lindevall (2016) that described the droughts from the oldest to the recent as follows. The 1981-1983 drought affected 2.46 million people in the Mozambique part of the basin, and our results also illustrate this drought as the one of the most severe drought affected the LRB and extremely affected the stations located in Mozambique. The 1983-1984 drought is also reported by Lindevall (2010) that coincides with our findings. Mozambique was severely affected by the drought, the impact of drought was aggravated by a cholera epidemic, which caused many deaths. The 1991-1992 drought was the most severe drought in southern Africa countries and more than 1.32 million people were severely affected including, residents of the LRB (Gebre and Getahum, 2016). The 1994-1995 drought affected many SADC countries, overcoming the 1991-1992 drought in some part of the basin. In Mozambique alone, more than 1.5 million people were affected. The region suffered a major agricultural failure. The 2002-2003 drought affected the region part of Mozambique in the basin. The 2005 drought affected parts of Mozambique and Zimbabwe, and very high temperature exacerbated the effects of the prolonged drought conditions impacted negatively on production and food security in the LRB. The 2015-2016 affected Southern Africa and resulted in parts of the LRB experiencing driest conditions. The drought affected Botswana and resulted in the dying up of the Gabarone Dam (the main water supply for Botswana's capital) located in the LRB and was declared as the worst drought in 3 decades in Botswana (Nonjinge, 2018).

Despite differences over space and time, our results here demonstrate that SPEI captures the main drought conditions over the study area that are reflected by other studies (example: Nonjinge, 2018) and can be used to study local drought-related processes and social impacts in Limpopo River Basin (Peng, 2020).

5.4. Trend analysis of drought

The analysis of drought trends and their spatial and temporal variability is vital to assess induced climate changes and suggest appropriate water resources and temporal management strategies for the future (Mahajan and Dodamani, 2015). In this study annual and seasonal SPEI timescales are investigated, based on the MK test and Sens's slope value. The results of large-scale SPEI trends suggest that all the stations

except station 1 (showing no significant decrease trend), patterns show decreasing trends over the study period from 1918 to 2018, with higher magnitude also seen for all the stations (except the station 1 having the lowest magnitude value), indicating that the study region as a whole is getting drier though the time. The SPEI 3-month timescale showed a negative trend for the majority of the stations during different seasons of the year. Winter is the driest season, with 8 stations having a significant decrease trend with the highest magnitude of change and Station 1 having an insignificant dry trend. The wet season in the LRB is summer, which had 89% of the stations with an insignificant decrease trend and station 11% (corresponding to station 1) having an insignificant wet trend.

The results of trend suggest that Station 1 located in Mozambique, is the moistest region over the study area, showing a slight wetting trend during summer and spring and an insignificant dry trend during autumn and winter and annual trend. According to FAO (2004), the Mozambique coastal plain where Station 1 is located is manly warm-temperate with no dry season and hot summers. This explains why in the annual and seasonal trend in this region does not show a significant dry trend over the period of analysis compared to other regions along the basin that are characterized by semi-arid, dry and hot climate. Additionally, Gebre (2016) reported that the lower Limpopo, where Station 1, is located is an area prone to flood. On the other hand, Stations 6 and 8, located in Botswana and South Africa, are the driest stations; they present a significant decrease trend in autumn, winter and spring.

Previous studies have also reported that in Africa drought events have tended to increase in recent years. For example, in the study of Dai (2011) on droughts and aridity in North America, China and Africa, the researcher reported that in Africa drought areas increased during the twentieth century and aridity trends are projected to increase continuously in the twenty-first century. In addition, Sheffield et al. (2012) reported that drought patterns have been increased over the last 60 years in Africa. The study of Masih et al. (2014) also suggested an increase of drought in Africa during the period of 1901-2011; the analysis was conducted based on the Spearman rank test, which is used to test statistical significance test on data.

5.5. Vegetation response to drought

According to Vicente-Serrano et al. (2012), the influence of drought on vegetation changes markedly with the season and between regions. Based on the

results of correlation between NDVI and SPEI, it is clear that the correlation between NDVI and SPEI varies according to SPEI timescale and the different location of the stations. The time-scale at which droughts affect vegetation provide information to understand how vegetation responds to drought (Vicente-Serrano et al., 2013). In this study, the highest correlation between NDVI and SPEI is found for SPEI 12-month timescale for the majority of the stations. According to Breshears et al., (2005) in semiarid regions vegetation tends to respond to drought at a longer timescale; in these regions vegetation is adapted to regularly tolerate periods of water deficit and has physiological mechanism to cope with these conditions. Long-term time series comparison of SPEI and NDVI from 2001 to 2018 suggest a positive and strong correlation between SPEI and NDVI for 89% of the stations. However, for the Station 1, the correlation between the two variables is too weak. According to Vicente-Serrano et al. (2012) the influence of the drought is lower in zones characterized by humid conditions. The lower Limpopo, where Station 1 is located, is such of that region; this explains why in this region the correlation between annual SPEI and NDVI is weak.

Seasonality should be an important factor for decision makers to consider when NDVI is employed in drought detection (Ji and Peters, 2003). In order to analyze how vegetation responds to drought based on the different seasons, the SPEI 3-month time scale was used. From the analysis of SPEI 3-month timescale and seasonal NDVI the results suggest a high correlation between SPEI and NDVI during autumn for all the stations, spring and summer for the majority of the stations. For winter, on the other hand, vegetation response seems to be insensitive to drought at 3-month time scale; the results have shown a weak but positive correlation for the majority of the stations with exception of one station 9. Something interesting happens to the station 9, which is in in the highest part of the basin with a temperate climate; during winter this station presents a negative correlation between SPEI and NDVI, this is probably due to the fact that the vegetation of the mountainous areas has different characteristics from other areas of the basin. The lower and negative correlation between NDVI and SPEI are probably due to complex physiological processes associated with vegetation and the fact that the state of the ecosystem is driven by multiple variables other than water availability (Peng et al., 2020). In overall, the results showed that plants in arid regions are able to respond very rapidly to small droughts periods.

Although the correlations between SPEI and NDVI is relatively low for some of the stations in summer, spring, and for the majority of the stations during winter, overall results of correlation between NDVI and SPEI suggest that SPEI has a positive correlation with NDVI, which is also reported by previous studies (Vicente-Serrano et al., 2012; Peng et al., 2020; Wang et al., 2020). The results indicate that the SPEI is one of the factors affecting NDVI change. This implies that SPEI values have an effect on the temporal change of NDVI.

The correlation between annual NDVI and annual SPEI over the study area shows that the impact of drought on vegetation based on SPEI values has a strong correlation. When SPEI values increase, NDVI values also tend to increase, and years with drought have a low NDVI value as well. A significant decrease of NDVI is registered during winter; this coincides with the values of strong severe drought that is also registered during the same period. Thus, according to Peng et al., (2020) results demonstrate that generated SPEI captures the main drought conditions that are reflected by low values of NDVI, and thus can be used to study regional drought-related processes and social impacts in the LRB. The annual SPEI indicate that longer timescales perform well in the correlation analysis between SPEI and NDVI, which is also reported by previous study (example: Vicente-Serrano, 2012; Törnros and Menzel, 2014).

Overall, the results suggest that the vegetation in semi-arid and humid zones of the basin are both affected by drought. The vegetation in semi-arid zones where the majority of the stations are located respond to drought in short and long term periods. While the vegetation in humid regions where Station 1 is located respond to drought in short periods, in these regions, plants generally have a low adaptability to water scarcity (Vicente-Serrano, 2013).

Knowledge of the period of time in which drought influences vegetation can be critical for early detection of vegetation damage, and can additionally be useful for identifying the response patterns that determine the resistance of various types of vegetation to drought (Vicente-Serrano, 2013). The time interval between rainfall and vegetation response differs between vegetation types and regions, and the capacity of soil to store water (Quiring and Ganesh, 2010). For further analysis, it would be nice to study how different types of vegetation respond to drought over the Limpopo River Basin.

5. Conclusion

The results of the analyses presented in this study show that the Standardized Precipitation Evapotranspiration Index is an important index that can be used to study the temporal and spatial patterns of droughts, and can recognize the characteristics of drought in the Limpopo River Basin. The results suggest that drought has become more frequent during the studied time period. The drought frequency analysis showed that drought events have a higher occurrence during the short-term drought (3-month SPEI), however for the long-term time-scale, these frequencies have been reduced but droughts become longer. The results of the frequency of drought onset and termination over the LRB in the past 100 years of analysis show that the characteristics of drought onset are essentially random in the basin, and there is no specific season in which drought tends to begin. However, the end of the drought is more likely to occur during spring and autumn.

In case of vegetation, in response to drought it is concluded that seasonal and annual SPEI correlates with values of NDVI. This implies that NDVI are important data that can be used for detecting droughts in the study area. Considering the short and long-term SPEI, the 12-month SPEI has the highest correlation with NDVI, therefore it is suggested that the 12-month SPEI is best for determining drought severity in vegetation for semi-arid regions as the LRB. Although the 12-month time scale suggest a high correlation between NDVI and SPEI, the results show that seasonality has a very significant effect on relationship between SPEI and NDVI.

The results from the Mann-Kendall trend tests and Sen's slope estimate revealed that both the annual and seasonal SPEI showed trends of aridity for all stations under the analysis, although the extent of the variation trend was diverse.

Reference

Abuzar, M. K., Amer, S., Fiza, M., Saleem, A. R., Malik, A. H., Khalil, T., & Shaista, S. (2017). Drought risk assessment using GIS and remote sensing : A case study of District Khushab, Pakistan. *15th International Conference on Environmental Science and Technology*, (September).

AghaKouchak, A., (2015). A multivariate approach for persistence-based drought prediction: application to the 2010–2011 East Africa drought.

AppEEARS Team. (2020). Application for Extracting and Exploring Analysis Ready Samples (AppEEARS). Ver. 2.49. NASA EOSDIS Land Processes Distributed Active Archive Center (LP DAAC), USGS/Earth Resources Observation and Science (EROS) Center, Sioux Falls, South Dakota, USA. Accessed November 17, 2020. https://lpdaacsvc.cr.usgs.gov/appeears

Bae, S., Lee, S. H., Yoo, S. H., & Kim, T. (2018). Analysis of drought intensity and trends using the modified SPEI in South Korea from 1981 to 2010. *Water (Switzerland)*, *10*(3).

Beguería, S., Vicente-Serrano, S. M., & Angulo-Martínez, M. (2010). A multiscalar global drought dataset: The SPEI base: A new gridded product for the analysis of drought variability and impacts. *Bulletin of the American Meteorological Society*, *91*(10), 1351–1356. https://doi.org/10.1175/2010BAMS2988.1

Beguería, S., Sergio M. Vicente-Serrano, F. R., & Latorre, B. (2014). *Standardized Precipitation Evapotranspiration Index (SPEI) revisited: parameter fitting, evapotranspiration models, tools, datasets and drought monitoring Santiago Beguería 1 , Sergio M. Vicente-Serrano 2, *, Fergus Reig 2 , Borja Latorre 1*. 1– 48.

Belal, A. A., El-Ramady, H. R., Mohamed, E. S., & Saleh, A. M. (2014). Drought risk assessment using remote sensing and GIS techniques. *Arabian Journal of Geosciences*, *7*(1), 35–53.

Boléo, José de Oliveira (1968), Moçambique, Pequena Monografia, Agência Geral do Ultramar, 3ª edição, Lisboa.

Breshears, D. D., Cobb, N. S., Rich, P. M., Price, K. P., Allen, C. D., Balice, R. G., … Meyer, C. W. (2005). Regional vegetation die-off in response to global-change-type drought. *Proceedings of the National Academy of Sciences of the United States of America*, *102*(42), 15144–15148.

Brito, R.; Famba, S; Munguambe, P.; Ibraimo, N. Julaia, C (2009) Profile of the Limpopo Basin in Mozambique. Integrated Water Resource Management for Improved Rural Livelihoods: Managing risk, mitigating drought and improving water productivity in the water scarce Limpopo Basin."

Bulpitt, C. J. (1967). Heparin as an Analgesic in Myocardial Infarction: A Double-blind Trial. *British Medical Journal*, *3*(5560), 279–281. https://doi.org/10.1136/bmj.3.5560.279

Chen, S., Zhang, L., Liu, X., Guo, M., & She, D. (2018). *The Use of SPEI and TVDI to Assess Temporal-Spatial Variations in Drought Conditions in the Middle and Lower Reaches of the Yangtze River Basin, China*. *2018*.

Chuvieco, E., & Huete, A. (2009). Fundamentals of satellite remote sensing. In *Fundamentals of Satellite Remote Sensing*. https://doi.org/10.1201/b18954

Didan, K. (2015). *MOD13A3 MODIS/Terra vegetation Indices Monthly L3 Global 1km SIN Grid V006*. NASA EOSDIS Land Processes DAAC. Accessed 2020-11-17 from https://doi.org/10.5067/MODIS/MOD13A3.006. Accessed November 17, 2020.

Dikshit, A., Pradhan, B., & Alamri, A. M. (2020). Short-term spatio-temporal drought forecasting using random forests model at New South Wales, Australia. *Applied Sciences (Switzerland)*, *10*(12). https://doi.org/10.3390/app10124254

FAO (2004), Drought impact mitigation and prevention in the Limpopo River Basin, Land and water discussion paper n.º 4, Rome.

FAO-SAFR (2004). *Drought Impact Mitigation and Prevention in the Limpopo River Basin* – A Situation Analysis. Sub-Regional Office for Southern Africa/Harare.Rome.

FAO. (2008). *The Near East drought planning Manual: Guidelines for drought mitigation and preparedness planning*.

Food and Agriculture Organization of the United Nations. (2016). *Drought characteristics and management in the Caribbean*. Retrieved from http://www.fao.org/3/a-i5695e.pdf

Fung, K. F., Huang, Y. F., & Koo, C. H. (2020). Assessing drought conditions through temporal pattern, spatial characteristic and operational accuracy indicated by SPI and SPEI: case analysis for Peninsular Malaysia. In *Natural Hazards* (Vol. 103). https://doi.org/10.1007/s11069-020-04072-y

Gebre, S. L., & Getahun, Y. S. (2016). *Analysis of Climate Variability and Drought Frequency Events on Limpopo River Basin, South Africa*. *7*(3). https://doi.org/10.4172/2157-7587.1000249

Gebremeskel, G., Tang, Q., Sun, S., Huang, Z., Zhang, X., & Liu, X. (2019). Droughts in East Africa: Causes, impacts and resilience. *Earth-Science Reviews*, *193*(July), 146–161. https://doi.org/10.1016/j.earscirev.2019.04.015

Giuseppe, E. Di, Pasqui, M., Magno, R., & Quaresima, S. (2019). *A Counting Process Approach for Trend Assessment of Drought Condition*. https://doi.org/10.3390/hydrology6040084

Ghosh, K. G. (2019). Spatial and temporal appraisal of drought jeopardy over the Gangetic West Bengal, eastern India. *Geoenvironmental Disasters*, *6*(1), 1–21. https://doi.org/10.1186/s40677-018-0117-1

Hassan, M.M., Smith, A.C., Walker, K., Rahman, M.K., Southworth, J., (2018). Rohingyarefugee crisis and forest cover change in Teknaf, Bangladesh. Rem. Sens.://doi.org/10.3390/rs10050689.

Haile, G. G. (2019). Droughts in East Africa : Causes, impacts and resilience Earth-Science Reviews *193*(April), 146–161. https://doi.org/10.1016/j.earscirev.2019.04.015

Heim, R.R., 2002: A review of twentieth-century drought indices used in the United States. *Bulletin of the American Meteorological Society,* **83**, 1149-1165.

International Fund for Agricultural Development (IFAD). 1996. *Review of research findings applicable to the dry communal areas of Zimbabwe.* Report No. 0657-ZI rev.1 of South Eastern Dry Areas Project and Smallholder Dry Areas Resource Management Project, Africa II Division, Programme Management Department. Rome.

International Federation of Red Cross and Red Crescent (IFRC). (2019). Immediate action needed as millions face hunger in Southern Africa, warns the Red Cross. Accessed September 01, 2020.

Iviescas, C. A. V. E. G. A., Rootveld, J. I. P. G., & Odríguez, E. R. A. R. (2019). *Testing the earth2observe datasets to compute the spi and the spei over the magdalena-cauca macrobasin in colombia*. *7119*, 3742–3749. https://doi.org/10.3850/38wc092019-1054

Jamro, S., Channa, F. N., Dars, G. H., Ansari, K., & Krakauer, N. Y. (2020). *applied sciences Exploring the Evolution of Drought Characteristics*.

Jenkerson, Calli; Maiersperger, Thomas; Schmidt, Gail. 2010. eMODIS: A User-Friendly Data Source; OFR; 2010-1055;

Ji, L., & Peters, A. J. (2003). Assessing vegetation response to drought in the northern Great Plains using vegetation and drought indices. *Remote Sensing of Environment*, *87*(1), 85–98. https://doi.org/10.1016/S0034-4257(03)00174-3

Kandji, S.T.; Verchot, L.; Mackensen, J. (2006). Climate Change Climate and Variability in Southern Africa: Impacts and Adaptation in the Agricultural Sector; UNEP;

Kendall, M.G., 1975. Rank Correlation Methods. Griffin, London, UK.

Khambhammettu, P. (2005). Mann-Kendall analysis for the Fort Ord Site. *HydroGeoLogic, Inc.*, 1–7.

Lee, S. H., Yoo, S. H., Choi, J. Y., & Bae, S. (2017). Assessment of the impact of climate change on drought characteristics in the Hwanghae Plain, North Korea using time series SPI and SPEI: 1981–2100. *Water (Switzerland)*, *9*(8). https://doi.org/10.3390/w9080579

Legesse Gebre, S., & Getahun, Y. S. (2016). Analysis of Climate Variability and Drought Frequency Events on Limpopo River Basin, South Africa. *Journal of Waste Water Treatment & Analysis*, *7*(3). https://doi.org/10.4172/2157-7587.1000249

Łabedzki, L. (2007). *Estimation of local drought frequency in central poland using the Standardized Precipitation Index SPI y*. *77*, 67–77.https://doi.org/10.1002/ird

Leira, E.M., Rafael, J., Bata, M.O., Mechisso, M., McNabb, M., Engelbrecht, R. Maló, S. 2002. Atlas for Disaster Preparedness and Response in the Limpopo Basin.

LI, X. xiang, JU, H., Sarah, G., YAN, C. rong, Batchelor, W. D., & LIU, Q. (2017). Spatiotemporal variation of drought characteristics in the Huang-Huai-Hai Plain, China under the climate change scenario. *Journal of Integrative Agriculture*, *16*(10), 2308–2322. https://doi.org/10.1016/S2095-3119(16)61545-9

Lindevall, E., DisasterRisk in a Changing Environment in the Lipopo River Basin. USGS. Acced at (https://www.arcgis.com/apps/Cascade/index.html?appid=22287abd11ce4afd82fb4 bfecbf11885 last access 19/12/2020).

Mahajan, D. R., & Dodamani, B. M. (2015). Trend Analysis of Drought Events Over Upper Krishna Basin in Maharashtra. *Aquatic Procedia*, *4*(Icwrcoe), 1250–1257. https://doi.org/10.1016/j.aqpro.2015.02.163

Makondo, C. C., & Thomas, D. S. G. (2020). Seasonal and intra-seasonal rainfall and drought characteristics as indicators of climate change and variability in Southern Africa: a focus on Kabwe and Livingstone in Zambia. *Theoretical and Applied Climatology*, *140*(1–2), 271–284. https://doi.org/10.1007/s00704-019-03029-x

Manhique, E. V. (2016). *impacto das mudanças climáticas sobre o rendimento do milho (zea mays) em sequeiro na bacia do rio limpopo universidade eduardo mondlane Faculdade de Agronomia e Engenharia Florestal Mestrado em Gestão de Solos e Água Limpopo*.

Mann, H.B., (1945). Nonparametric tests against trend. Econometrica 13.

Masih, I., & Maskey, S. (2014). *A review of droughts on the African continent : a geospatial and long-term perspective*. (October). https://doi.org/10.5194/hess-18-3635-2014

Merz, L., Yang, D., & Hull, V. (2020). A metacoupling framework for exploring transboundary watershed management. *Sustainability (Switzerland)*, *12*(6), 1–16. https://doi.org/10.3390/su12051879

Mishra, A. K. and Singh, V. P.: A review of drought concepts, J. Hydrol.,391, 202–216, doi:10.1016/j.jhydrol.2010.07.012, 2010.

Milhano, Ana Paula Ferreira Ribeiro da Costa - Gestão dos recursos hídricos em Moçambique: Gaza – rio Limpopo [Em linha]. Lisboa: ISCTE, 2008. Tese de mestrado.

Mo, K. C. (2011). Drought onset and recovery over the United States, J. Geophys. Res., 116, D20106, doi:10.1029/2011JD016168.

Mo, K. C., & Lyon, B. (2015). Global meteorological drought prediction using the North American multi-model ensemble. *Journal of Hydrometeorology*, *16*(3), 1409–1424. https://doi.org/10.1175/JHM-D-14-0192.1

Mosase, E., & Ahiablame, L. (2018). *Rainfall and Temperature in the Limpopo River Basin, Southern Africa: Means, Variations, and Trends from 1979 to 2013*. https://doi.org/10.3390/w10040364

Nanzad, L., Zhang, J., Tuvdendorj, B., & Nabil, M. (2019). NDVI anomaly for drought monitoring and its correlation with climate factors over Mongolia from 2000 to 2016 NDVI anomaly for drought monitoring and its correlation with climate factors over Mongolia from 2000 to 2016. *Journal of Arid Environments*, *164*(March), 69–77. https://doi.org/10.1016/j.jaridenv.2019.01.019

NASA (2019) Drought Threatens Millions in Southern Africa. (https://earthobservatory.nasa.gov/images/146015/drought-threatens-millions-in-southern-africa. Last access September, 2020)

Pathak, A. A., & Dodamani, B. M. (2019). Comparison of Meteorological Drought Indices for Different Climatic Regions of an Indian River Basin. *Asia-Pacific Journal of Atmospheric Sciences*, (2010). https://doi.org/10.1007/s13143-019-00162-5

Peng, J., Dadson, S., Hirpa, F., Dyer, E., Lees, T., Miralles, D. G., Funk, C. (2020). A pan-African high-resolution drought index dataset. *Earth System Science Data*, *12*(1), 753–769. https://doi.org/10.5194/essd-12-753-2020

Pohlert, T. (2020). *Non-Parametric Trend Tests and Change-Point Detection*. 1–18.

Quiring, S. M., and S. Ganesh (2010), Evaluating the utility of the Vegetation Condition Index (VCI) for monitoring meteorological drought in Texas, Agric. For. Meteorol. doi:10.1016/j.agrformet. 2009.11.015.

SADCC (1992). Food Security Bulletin, Gaborone, Botswana: SADC. Sandford

Schwab, J. C. (2013). Planning and Drought. *American Planning Association: Planning Advisory Service*, (Report Number 574), 100. Retrieved from http://drought.unl.edu/Planning/PlanningProcesses/PlanningandDrought.aspx

Shah, D., & Mishra, V. (2020). *Drought Onset and Termination in India Drought Onset and Termination in India*. (July). https://doi.org/10.1029/2020JD032871

Sönmez, F. K., Kömüscü, A. Ü., Erkan, A., & Turgu, E. (2005). An analysis of spatial and temporal dimension of drought vulnerability in Turkey using the standardized precipitation index. *Natural Hazards*, *35*(2), 243–264. https://doi.org/10.1007/s11069-004-5704-7

Stagge, J. H., Tallaksen, L. M., Gudmundsson, L., Van Loon, A. F., & Stahl, K. (2015). Candidate Distributions for Climatological Drought Indices (SPI and SPEI). *International Journal of Climatology*, *35*(13), 4027–4040. https://doi.org/10.1002/joc.4267

Thornthwaite, C.W., 1948: An approach toward a rational classification of climate. Geographical Review.

Tong, S., Lai, Q., Zhang, J., Bao, Y., Lusi, A., Ma, Q., Zhang, F. (2018). Spatiotemporal drought variability on the Mongolian Plateau from 1980–2014

based on the SPEI-PM, intensity analysis and Hurst exponent. *Science of the Total Environment*, *615*, 1557–1565. https://doi.org/10.1016/j.scitotenv.2017.09.121

Törnros, T., & Menze, L. (2014). *Addressing drought conditions under current and future climates in the Jordan River region.* (March 2016). https://doi.org/10.5194/hess-18-305-2014

Trambauer, P., Werner, M., Winsemius, H. C., Maskey, S., Dutra, E., & Uhlenbrook, S. (2015). Hydrological drought forecasting and skill assessment for the Limpopo River basin, southern Africa. *Hydrology and Earth System Sciences*, *19*(4), 1695–1711. https://doi.org/10.5194/hess-19-1695-2015

Van der Schrier, G., P. D. Jones, and K. R. Briffa (2011), The sensitivity of the PDSI to the Thornthwaite and Penman-Monteith parameterizations for potential evapotranspiration, J. Geophys. Res., 116, D03106, doi:10.1029/2010JD015001

Vicente-Serrano, S. M., Begueria, S., & López-Moreno, J. I. (2010). a multi-scalar drought index sensitive to global warming: the standardized precipitation evapotranspiration index – *SPEI*. https://doi.org/10.1175/2009JCLI2909.1

Vicente-Serrano, S.M., Beguería, S., López-Moreno, J.I., Angulo, M., El Kenawy, A. (2010): A new global 0.5° gridded dataset (1901-2006) of a multiscalar drought index: comparison with current drought index datasets based on the Palmer Drought Severity Index. *Journal of Hydrometeorology.*

Vicente-Serrano, S. M., Gouveia, C., Camarero, J. J., Beguería, S., Trigo, R., López-Moreno, J. I., … Sanchez-Lorenzo, A. (2013). Response of vegetation to drought time-scales across global land biomes. *Proceedings of the National Academy of Sciences of the United States of America*, *110*(1), 52–57. https://doi.org/10.1073/pnas.1207068110

Vicente-Serrano, S. M., Gouveia, C., Camarero, J. J., Beguería, S., Trigo, R., López-Moreno, J. I., … Sanchez-Lorenzo, A. (2012). *drought impacts on vegetation activity , growth and primary production in humid and arid ecosystems.*

World Meteorological Organization (WMO). (2012). *Limpopo River Basin: A proposal to improve the flood forecasting and early warning systems*. 47.

Wang, Z., Li, J., Lai, C., Huang, Z., Zhong, R., Zeng, Z., & Chen, X. (2018). Increasing drought has been observed by SPEI_pm in Southwest China during 1962–2012. *Theoretical and Applied Climatology*, *133*(1–2), 23–38. https://doi.org/10.1007/s00704-017-2152-3

Wang, F., Wang, Z., Yang, H., & Zhao, Y. (2018). Study of the temporal and spatial patterns of drought in the Yellow River basin based on SPEI. *Science China Earth Sciences*, *61*(8), 1098–1111. https://doi.org/10.1007/s11430-017-9198-2

Wang, Y., Zhang, C., Meng, F., Bourque, C., Zhang, C. (2020). Evaluation of the suitability of six drought indices in naturally growing, transitional vegetation zones in Inner Mongolia (China)

Wilhite D. A, Glantz MH (1987). Understanding the drought phenomena: the role of definitions. In: Wilhite DA, Easterling WE, Deobarah A (eds) Planning of drought: towards a reduction of societal vulnerability.

Wilhite DA (2000). Drought as a Natural Hazard: Concepts and Definitions.

Wilhite, D. A. (2016). Managing drought risk in a changing climate. *Climate Research*, *70*(2–3), 99–102. https://doi.org/10.3354/cr01430

Yevjevich, V., 1967. An objective approach to definitions and investigations of continental hydrologic, droughts. Hydrol. Pap. Colorado State University, Fort Collins.

Zhang, L., Wang, Y., Chen, Y., Bai, Y., & Zhang, Q. (2020). Drought risk assessment in central Asia using a probabilistic copula function approach. *Water (Switzerland)*, *12*(2). https://doi.org/10.3390/w12020421

Zhu, T., & Ringler, C. (2010). Climate Change Implications for Water Resources in the Limpopo River Basin. *Food Policy*, (April), 16. Retrieved from http://www.ifpri.org/publication/climate-change-implications-water-resources-limpopo-river-basin

APPENDIX

```
"""
        Program developed by: Sandra Sambo in cooperation with Márcio Mathe.
07/10/2020
        The program calculates the drought characteristics based on SPEI time series:
The following characteristics can be calculated using the program: drought onset,
termination, severity, intensity and frequency
"""


import csv
import numpy as np
import math
import pandas as pd


import csv
with open('D:/Master/1. master
Thesis/NGEM01/SPEI_EXCEL/data/station_1_3_month.csv', 'r') as csvfile:
    reader = csv.reader(csvfile, delimiter=';', quotechar='"')
    data=list(reader)
# add dummy data in order to process include all the months with drought in the
dataset
    iiii=['dummy','9999999']
    data.append(iiii)
    del data[0] #deletes the column names row
    del data[0:206] #delete years from 1901 to 1917



#realdata = [] #indexes list without the dates
tt=0
periods = []
epochs = []
month = []
month_temporary = []
#negdata = [] #negative values from realdata
```

```
for row in data:
    if float(row[1]) < -0.5:          # thereshold of 0
        epochs.append(row)
    else:
        if(len(epochs) > 0):
            periods.append(epochs)
            epochs = []
print('epochs',periods)


if (len(periods) > 0):
    yy = []
    ranges = []
    severity_temporary=[]
    severity=[]
    duration_temporary=[]
    duration=[]
    monthsuu=[]
    intensity_temporary=[]
    intensity=[]


    for row in periods:
        y = []
        ranges.append(str(row[0][0]) + ' - ' + str(row[len(row) - 1][0]))
        for subrow in row:
            y.append(abs(float(subrow[1])))
        yy.append(y)

    # nr of Month
    for row in periods:
        x = 0
        months = []
        for subrow in row:
            x = x + 1
```

```python
        months.append(x)
        monthsuu.append(months)


#Drought severity
    for row in yy:
        severity_temporary.append(math.fsum(row))
    l = 0
    for row in severity_temporary:
        severity.append([ranges[l], row])
        l += 1
    ww = 0


    duration = []
    for sublist in monthsuu:
        for item in sublist:
            duration.append(item)


    for i in range(len(duration)):
        intensity_temporary = (severity_temporary[i] / duration[i])
        intensity.append(intensity_temporary)


    # dictionary of lists


    dict = {'onset_termination': ranges, 'duration': duration,
        'severity': severity_temporary, 'Intensity': intensity}


    df = pd.DataFrame(dict)


    print(df)
    df.to_csv(r'D:\Master\1. master
Thesis\NGEM01\SPEI_EXCEL\Results_drought_characteristics\Station_1_3_month.
csv',
        index=False, header=True)
```

```
# number of drought events per type of drought (Drought frequency)
Extreme_drought=0;
severe_drought=0;
moderate_drought=0;
mild_drought=0;
non_drought=0;


for row in data:
    if float(row[1]) <= -2 and float(row[1]) >= -5:   #to exclude the dummy data
        Extreme_drought=Extreme_drought+1
    elif float(row[1]) <=-1.5 and float(row[1])> -1.999999:
        severe_drought=severe_drought+1
    elif float(row[1]) <=-1 and float(row[1])>-1.499999:
        moderate_drought=moderate_drought+1
    elif float(row[1]) <=-0.5 and float(row[1])> -0.999999:
        mild_drought=mild_drought+1
    elif float(row[1])>-0.5:   # to exclude dummy data
        non_drought=non_drought+1
total=Extreme_drought+severe_drought+moderate_drought+mild_drought+non_drou
ght+2
total_m=0
total_months=0
for row in data:
    total_m=total_m+1
total_months=total_m-2+2   #exclude dummy data
# Drought Frequency
# frequency of extreme drought
freq_extreme_drought=float((float(Extreme_drought)/float(total_months))*100)
# frequency of severe drought
freq_severe_drought=float((float(severe_drought)/float(total_months))*100)
# frequency of Moderate drought
freq_moderate_drought=float((float(moderate_drought)/float(total_months))*100)
# frequency of Mild drought
freq_mild_drought=float((float(mild_drought)/float(total_months))*100)
```

```
timescale=3
nr_of_year=100


"""
number of droughts per 100 years was calculated as:
Ni,100=(Ni/i.n)*100
where Ni,100 the number of droughts for a timescale i in 100 years
Ni the number of months with droughts for a timescale i in the n-year set
i timescale ( 3, 6, 12, 24, 48 months)
n the number of years in the data set ( 100)
"""
# number of droughts per 100 years
freq_extreme= float((float(Extreme_drought)/(timescale*float(nr_of_year))*100))
freq_severe= float((float(severe_drought)/(timescale*float(nr_of_year))*100))
freq_moderate= float((float(moderate_drought)/(timescale*float(nr_of_year))*100))
freq_mild=float((float(mild_drought)/(timescale*float(nr_of_year))*100))


print ('extreme drought in 100 years', freq_extreme)
print ('severe drought  in 100 years',freq_severe)
print ('moderate drought  in 100 years', freq_moderate)
print ('mild drought in 100 years', freq_mild)
```

Appendix 1. python program used for the calculation of the characteristics of drought.
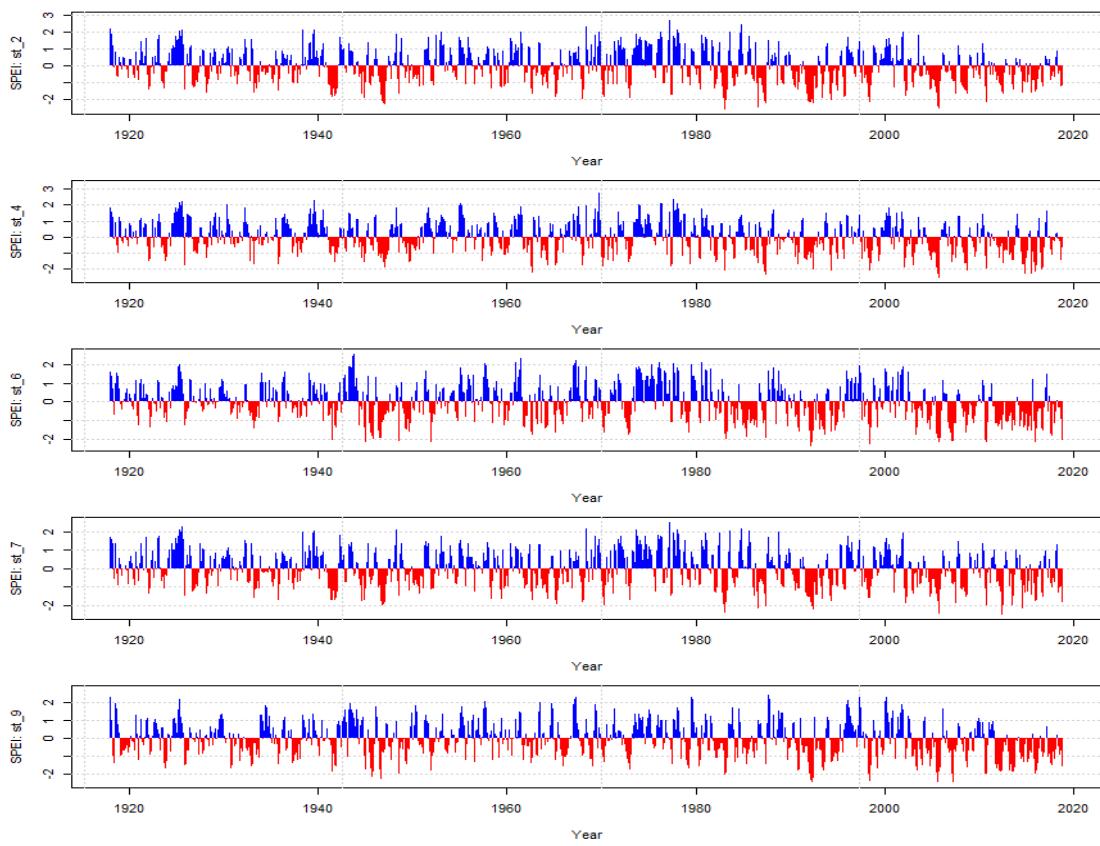
Appendix 2. Temporal variability of the SPEI at 3-month-scale from 1918-2018 (stations 2, 4, 6 and 9 respectively)
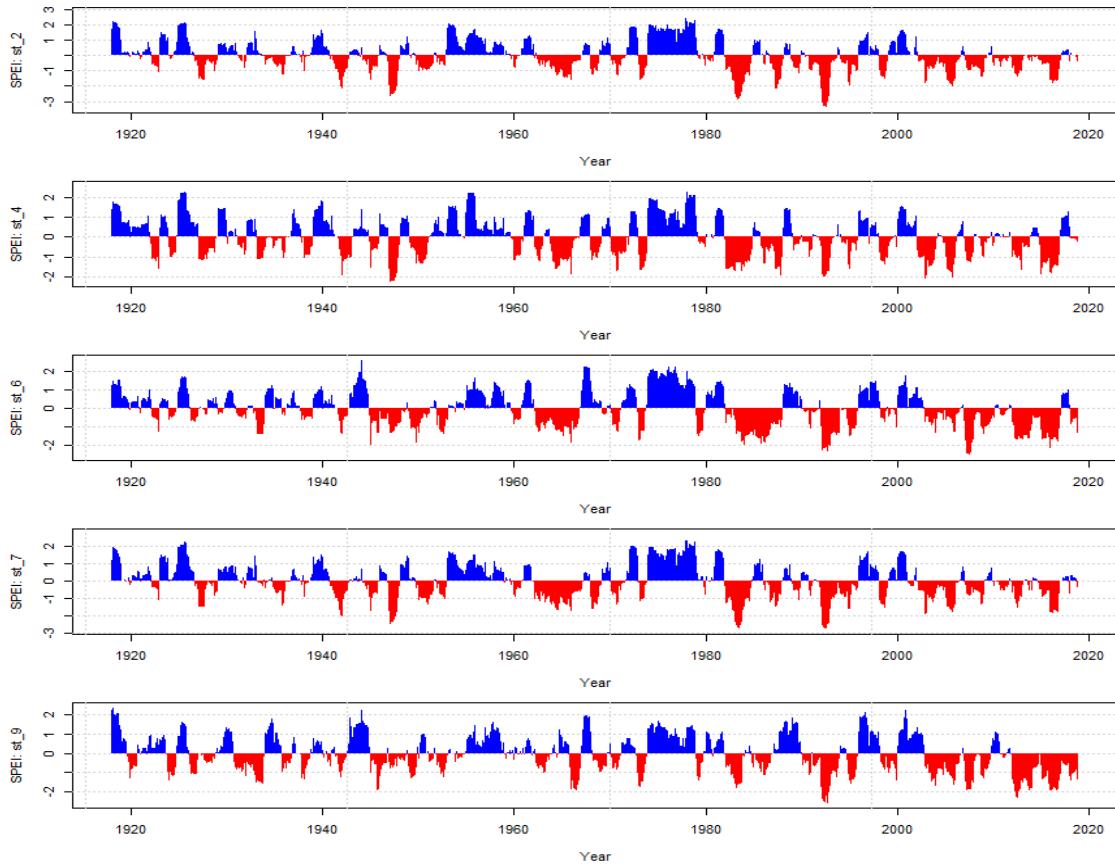
Appendix 3. Temporal variability of the SPEI at 12-month-scale from 1918-2018 (stations 2, 4, 6 and 9 respectively)

Appendix 4. Drought Frequency

| Countries	lag-time	Station	latitude	longitude	Mild drought (<=-0.5 to -0.99)	Moderate drought (-1 to -1.49)	Severe drought (-1.5 to -1.99)	Extreme drought (<-2.0)	Total number of droughts
Mozambique		Station_1	24°45'15.1"S	33°37'8.8"E	67	43	20	7	137
		Station_2	22°36'41.5"S	31°42'10.5"E	61	49	20	9	139
Zimbabwe		Station_3	21°45'28.6"S	30°39'27.8"E	63	40	28	5	136
		Station_4	20°51'7.6"S	28°18'21.7"E	66	44	23	6	139
Botswana	3- month	Station_5	22°14'44.5"S	27°43'52.2"E	65	43	27	5	140
		Station_6	24°10'45.6"S	26°13'58.9"E	57	53	22	8	140
South Africa		Station_7	23°15'21.8"S	30°44'41.4"E	67	47	25	5	144
		Station_8	23°49'51.3"S	28°44'29.5"E	70	45	27	6	148
		Station_9	26°7'49.3"S	29°14'48.1"E	68	44	24	5	141
Mozambique		Station_1	24°45'15.1"S	33°37'8.8"E	15	10	4	3	32
		Station_2	22°36'41.5"S	31°42'10.5"E	18	8	4	3	33
Zimbabwe		Station_3	21°45'28.6"S	30°39'27.8"E	14	10	5	3	32
		Station_4	20°51'7.6"S	28°18'21.7"E	13	14	6	1	34
Botswana	12-month	Station_5	22°14'44.5"S	27°43'52.2"E	15	14	3	2	34
		Station_6	24°10'45.6"S	26°13'58.9"E	15	12	5	2	34
South Africa		Station_7	23°15'21.8"S	30°44'41.4"E	17	10	4	2	33
		Station_8	23°49'51.3"S	28°44'29.5"E	17	12	5	2	36
		Station_9	26°7'49.3"S	29°14'48.1"E	18	12	5	2	37

Appendix 5. Man-Kendall trend test, Sen's slope and p value of the 3- and 12-month SPEI time scale.

		trend is not significant if p-value > alfa(0.05)null hypothese
		Summer	Autumn	Winter	Spring	Annual
Stataion_1	ZS	0.77170	-1.29990	-0.75997	0.13204	0.58391
	p_value	0.44030	0.19360	0.44730	0.89500	0.5593
	sen slope	0.00297	-0.00484	-0.00307	0.00028	-0.001796
Stataion_2	ZS	-1.09150	-1.76050	**-2.93730**	-0.65726	**-2.2623**
	p_value	-0.07388	0.07832	0.00331	0.51100	0.02368
	sen slope	-0.00365	-0.00720	-0.01069	-0.00247	-0.008312
Stataion_3	ZS	-1.48770	-1.52290	**-3.56520**	-1.25880	**-2.7435,**
	p_value	0.13680	0.12780	0.00036	0.20810	0.006079
	sen slope	-0.00473	-0.00560	-0.01282	-0.00488	-0.009494
Stataion_4	ZS	-1.34680	-0.74237	**-4.55440**	-0.07336	**-2.1655**
	p_value	0.17800	0.45790	0.00001	0.94150	0.03035
	sen slope	-0.00489	-0.00258	-0.01578	-0.00026	-0.00836
Stataion_5	ZS	-1.12670	-1.54050	**-4.64320**	-0.98883	**-2.456**
	p_value	0.25990	0.12340	0.00000	0.32270	0.01405
	sen slope	-0.00435	-0.00558	-0.01648	-0.00357	-0.009057
Stataion_6	ZS	-0.99764	**-1.99820**	**-3.77070**	**-2.03340**	**-2.4383**
	p_value	0.31850	0.04569	0.00016	0.04201	0.01476
	sen slope	-0.00332	-0.00760	-0.01293	-0.00774	-0.00937
Stataion_7	ZS	-0.84505	-1.81040	**-2.97530**	-0.49002	**-2.2388**
	p_value	0.39810	0.07023	0.00293	0.62410	0.02517
	sen slope	-0.00279	-0.00715	-0.01062	-0.00194	-0.007266

		Annual	Summer	Autumn	Winter	Spring
	ZS	-0.62499	**-2.40900**	**-3.24820**	**-2.09500**	**-2.5997**
Stataion_8	p_value	0.53200	0.01600	0.00116	0.03617	0.00933
	sen slope	-0.00219	-0.00894	-0.01221	-0.00812	-0.009522
	ZS	-0.81277	-1.85740	**-2.07450**	-1.66660	**-2.0569**
Stataion_9	p_value	0.41630	0.06326	0.03803	0.09559	0.0397
	sen slope	-0.00296	-0.00687	-0.00723	-0.00617	-0.00807

Values in bold represent a significant trend in the data (p-value <0.05)
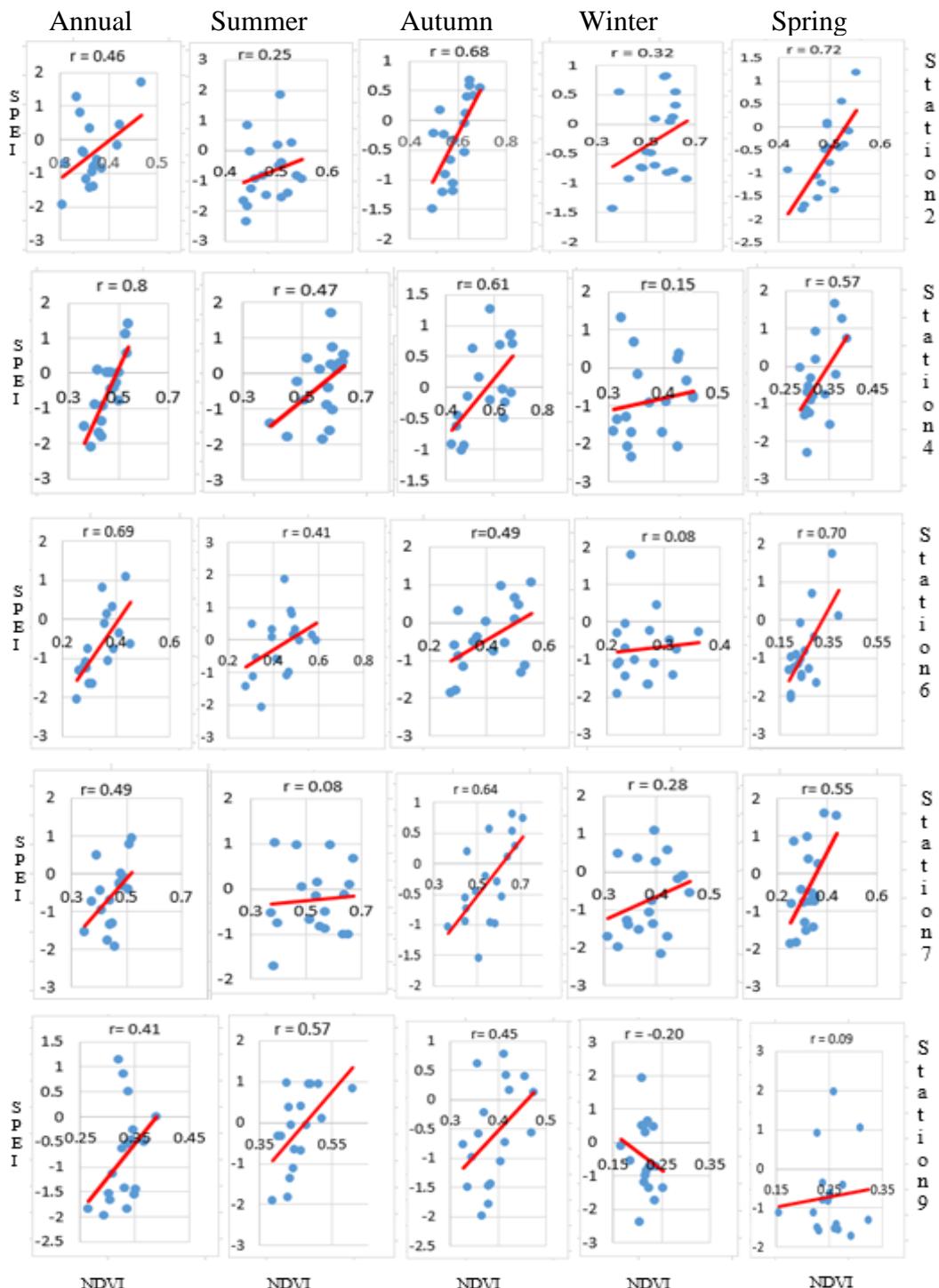
Appendix 6. Correlation between NDVI and SPEI for the stations 2,4,6,7 and 9